Monatsh Chem (2015) 146:15–33
DOI 10.1007/s00706-014-1302-x

ORIGINAL PAPER

Synthesis, spectral, X-ray diffraction, antimicrobial studies, and DNA binding properties of binary and ternary complexes of pentadentate N_2O_3 carbohydrazone ligands

Magdy Shebl · Saied M. E. Khalil

Received: 13 May 2014 / Accepted: 13 August 2014 / Published online: 23 September 2014

Abstract Two pentadentate carbohydrazone ligands, H_2L^1 and H_2L^2, were prepared by the reaction of the bifunctional compound carbohydrazide with 2-hydroxy-5-nitrobenzaldehyde and 2-hydroxy-1-naphthaldehyde, respectively. Reactions of the ligands with oxovanadium(IV), cerium(III), thorium(IV), and dioxouranium(VI) ions yielded binary complexes. Reactions of the ligands with the dioxouranium(VI) ion in the presence of secondary ligands (8-hydroxyquinoline, glycine, salicylaldehyde, or benzoylacetone) yielded ternary complexes. The ligands and metal complexes were characterized by different techniques such as elemental and thermal analyses, IR, ^{1}H and ^{13}C NMR, electronic, ESR, mass spectra, and powder XRD as well as magnetic susceptibility and conductivity measurements. The coordinating sites are phenolic oxygen, azomethine nitrogen, and carbonyl oxygen. In complexes, the ligands act as dibasic pentadentate except ternary dioxouranium(VI) complexes, obtained using glycine or benzoylacetone, in which the ligands act as monobasic pentadentate. The XRD patterns for the H_2L^1 ligand, its binary dioxouranium(VI) complex, and its 8-hydroxyquinoline ternary complex indicate crystalline nature and the grain size was estimated. The H_2L^1 ligand and its binary complex have triclinic systems while the ternary complex has a monoclinic system with different unit-cell parameters. The ligands and some of their metal complexes showed antimicrobial activity toward some Gram-positive and Gram-negative bacteria, yeast (*Candida albicans*), and fungus (*Aspergillus fumigatus*), and MIC values were determined. The DNA binding properties of the oxovanadium(IV) complexes of H_2L^1 and H_2L^2 ligands were investigated by electronic absorption spectroscopy and viscosity measurements. The results indicated that these complexes bind to DNA via an intercalation binding mode with an intrinsic binding constant K_b of 2.55×10^4 and 3×10^4 M^{-1}, respectively.

Keywords Carbohydrazones · Binary and ternary complexes · Pentadentate ligands · Antimicrobial activity · Powder XRD · DNA binding

Introduction

Carbohydrazide is a member of the structural sequence, urea, semicarbazide, and carbohydrazide. Both hydrazine groups of carbohydrazide display reactivity toward carbonyl compounds and give rise to a large number of crystalline mono- and dihydrazones. Carbohydrazones and their complexes with transition metals have been found to be one of the most fascinating subjects in the field of coordination chemistry as they are documented in the literature as good therapeutic, antimicrobial, anticancer, and pharmacological agents [1–6].

It is well known that the mixed-ligand strategy, as an effective method for constructing metal–organic frameworks, allows tuning the coordination ability of ligands to corporately bind with metal centers. Mixed-ligand complexes have been extensively studied following recognition that they play an important role in biological processes and serve as suitable models for valuable information in the elucidation of enzymatic processes of biological relevance

Electronic supplementary material The online version of this article (doi:10.1007/s00706-014-1302-x) contains supplementary material, which is available to authorized users.

M. Shebl (✉) · S. M. E. Khalil
Department of Chemistry, Faculty of Education, Ain Shams University, Roxy, Cairo, Egypt
e-mail: magdy_shebl@hotmail.com

[7, 8]. Also, these complexes showed significant antibacterial, antifungal, and anticancer activity [9–15].

Vanadium complexes have multiple biological and pharmacological activities, including antimicrobial, antileukemia, antitumor, photodynamic therapy, and as an insulin mimetic [16–20].

The coordination chemistry of lanthanide and actinide ions with O- and/or N-donor ligands has advanced tremendously during past two decades [21–24]. The considerable interest of these ions, especially lanthanide ions, is due to their implications in optical imaging of cells, as luminescent chemosensors for medical diagnostics, contrast reagents for medical magnetic resonance imaging, shift reagents for NMR spectroscopy as well as their increasing utility in organic synthesis, bioorganic chemistry, and homogeneous catalysis [25, 26].

Deoxyribonucleic acid, DNA, plays a fundamental role in the storage and expression of genetic information in a cell. DNA is a particularly good target for metal complexes as its base pairs own rich electrons. Therefore, transition metal complexes can bind to DNA in many modes such as electrostatic, groove, and intercalative binding. Among them, the intercalative mode is the most important mode in which transition metal complexes can intercalate between the pair-bases of double helix DNA, forming π–π overlapping interaction. It is this interaction that greatly affects and/or damages DNA conventional behavior and so that these transition metal complexes possess a very broad application background in the field of bio-inorganic chemistry [27–29]. Hence, studies of the interaction between transition metal complexes and DNA have been pursued in recent years [30–33], particularly oxovanadium(IV) complexes, which can bind and cleave DNA [34–37].

The aim of the present work is to study the chelating behavior of the carbohydrazone ligands (Fig. 1) toward oxovanadium (IV), lanthanide [cerium (III)] and actinide [thorium (IV) and dioxouranium(VI)] ions. Also, the ligands were allowed to react with the dioxouranium(VI) ion in the presence of secondary ligands including N,O-donor (8-hydroxyquinoline or glycine) or O,O-donor (salicylaldehyde or benzoylacetone). The structures of the ligands and metal complexes were characterized by elemental and thermal analyses, IR, ^{1}H and ^{13}C NMR, ESR, electronic, mass spectra, and powder XRD as well as conductivity and magnetic susceptibility measurements at room temperature. The biological activity of the ligands and their complexes was screened against selected kinds of bacteria and fungi. Finally, the interaction between the oxovanadium(IV) complexes and herring sperm DNA (HS-DNA) was investigated by electronic absorption spectroscopy and viscosity measurements.

Results and discussion

The carbohydrazone ligands H_2L^1 and H_2L^2

The carbohydrazone ligands 2,2′-[carbonylbis(hydrazin-2-yl-1-ylidenemethylidyne)]bis(4-nitrophenol) (H_2L^1) and 1,1′-[carbonylbis(hydrazin-2-yl-1-ylidenemethylidyne)]bis (naphthalen-2-ol) (H_2L^2) (Fig. 1) were synthesized by the condensation of carbohydrazide with 2-hydroxy-5-nitrobenzaldehyde and 2-hydroxy-1-naphthaldehyde, respectively, stoichiometrically in the molar ratio 1:2 (carbohydrazide:aldehyde). The structures of the ligands were elucidated by elemental analyses, IR, electronic, ^{1}H and ^{13}C NMR, and mass spectra. The analytical and physical data of the ligands and their metal complexes are listed in Table S1 (Supplementary material). The results of the elemental analyses are in a good agreement with the proposed formulae.

Inspection of the infrared spectral data of the carbohydrazone ligands H_2L^1 and H_2L^2 along with carbohydrazide showed the formation of the ligands. The absorption bands of the $–NH_2$ group in carbohydrazide disappeared in the infrared spectra of the ligands, indicating that the condensation has occurred. This is supported

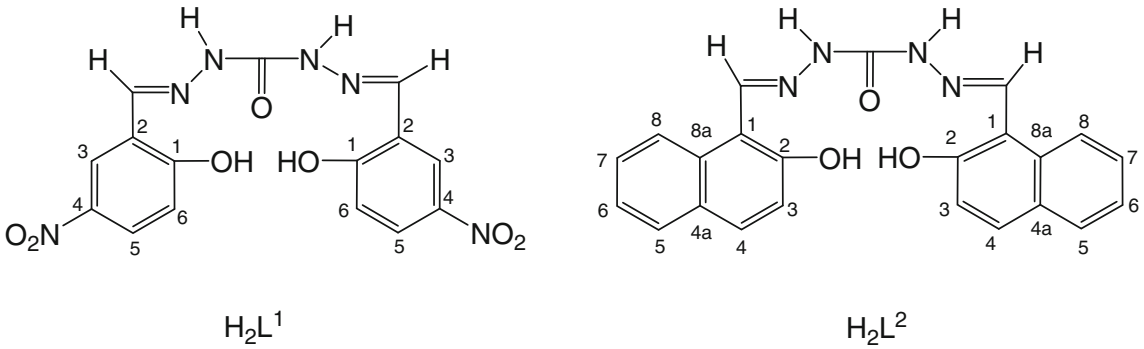

Fig. 1 Structures of the carbohydrazone ligands H_2L^1 and H_2L^2

by the appearance of the strong bands in the range 1,622–1,631 cm^{-1} in the spectra of the ligands, which can be assigned to the stretching mode of the azomethine moiety, ν(C=N). Also, the new broad bands at 3,431 and 3,323 cm^{-1} can be assigned to ν(OH) in H_2L^1 and H_2L^2 ligands, respectively. Also, the bands observed at 3,275, 1,674, 1,579, and 1,283 cm^{-1} in H_2L^1 ligand and 3,212, 1,676, 1,555, and 1,325 cm^{-1} in H_2L^2 ligand can be assigned to ν(NH), ν(C=O), ν(C=C), and ν(C–O)phenolic, respectively.

Electronic spectral data of the ligands (Table 1) were recorded in DMF solution. Five absorption bands at 279, 296, 352, 384, and 448 nm for the former ligand (H_2L^1) and 270, 292, 350, 385, and 420 nm for the latter one (H_2L^2) were observed and characterized. The first and third bands correspond to $^1L_a \rightarrow {}^1A_1$ and $^1L_b \rightarrow {}^1A_1$ transitions of the phenyl ring [38], and the second band corresponds to the $\pi \rightarrow \pi^*$ transition of the C=O group. The fourth band corresponds to the $\pi \rightarrow \pi^*$ transition of the azomethine group and the fifth band corresponds to the $n \rightarrow \pi^*$ transitions from the phenyl ring to the azomethine group [39].

^{1}H NMR spectra of the ligands were recorded in DMSO-d_6 with reference to TMS. Figure S1 (Supplementary material) depicts the ^{1}H and ^{13}C NMR spectra of the H_2L^1 ligand. ^{1}H NMR spectral data of the ligands exhibited three signals in the ranges 11.91–12.06, 10.64–11.24, and 7.09–9.22 ppm, which may be assigned to OH, NH, and HC=N protons, respectively. The aromatic protons were observed in the range of 7.23–8.72 ppm. Assignment of the ^{13}C NMR spectral data of the ligands is based on ^{13}C shifts in similar hydrazone ligands [38, 40]. The signals observed at 163.72 and 153.66 ppm in H_2L^1 ligand and 156.7 and 151.62 ppm in H_2L^2 ligand can be assigned to C=O and C=N, respectively. Aromatic carbon atoms were detected at appropriate shifts for both ligands.

The mass spectra of the H_2L^1 and H_2L^2 ligands (Fig. S2, Supplementary material) showed the molecular ion peaks at $m/z = 388$ and 398, respectively, confirming their formula weights (388.30 and 398.42, respectively). The mass fragmentation pattern, shown in Scheme S1 (Supplementary material), supported the suggested structure of the H_2L^1 ligand.

Characterization of the metal complexes

Reactions of oxovanadium(IV), cerium(III), thorium(IV), and dioxouranium(VI) ions with the carbohydrazone ligands H_2L^1 and H_2L^2 yielded binary complexes. Reactions of the ligands with the dioxouranium(VI) ion in the presence of secondary ligands (L′) [8-hydroxyquinoline (8-HQ), glycine (Gly), salicylaldehyde (Sal), or benzoylacetone (Bac)] yielded ternary complexes. The isolated metal complexes were identified by elemental and thermal analyses, IR, ^{1}H and ^{13}C NMR, electronic, ESR, and mass

Table 1 Electronic spectra, magnetic moments, and molar conductivity data of the carbohydrazone ligands H_2L^1 and H_2L^2 and their metal complexes

No.	Complex	Electronic spectral bands[a]/nm	μ_{eff}/BM	Conductance[a]/Ω^{-1} cm^2 mol^{-1}
	H_2L^1	279 (0.39), 296 (0.38), 352 (0.4), 384 sh (0.29), 448 (0.26)	–	–
1	$[(L^1)VO]\cdot 4H_2O$	548[b]	1.42	15
2	$[(L^1)Ce(EtOH)]NO_3\cdot EtOH$	502[b]	2.00	71
3	$[(L^1)Th(NO_3)_2]\cdot EtOH\cdot H_2O$	452[b]	Diam.	41.7
4	$[(L^1)UO_2]\cdot 2MeOH$	509[b]	Diam.	4
5	$[(L^1)UO_2(8\text{-HQ})]$	510[b]	Diam.	6
6	$[(HL^1)UO_2(Gly)]\cdot 0.5MeOH$	508[b]	Diam.	Insol.
7	$[(L^1)UO_2(Sal)]\cdot 4H_2O$	506[b]	Diam.	Insol.
8	$[(HL^1)UO_2(Bac)]\cdot MeOH$	455[b]	Diam.	Insol.
	H_2L^2	270 (0.39), 292 (0.36), 350 (0.41), 385 (0.27), 420 sh (0.27)	–	–
9	$[(L^2)VO]\cdot 3H_2O$	541[b]	1.00	18
10	$[(L^2)Ce(NO_3)]\cdot 2.5H_2O$	521[b]	2.06	18
11	$[(L^2)Th(NO_3)_2]\cdot 4H_2O$	460[b]	Diam.	42.3
12	$[(L^2)UO_2]\cdot 2H_2O$	465[b]	Diam.	16
13	$[(L^2)UO_2(8\text{-HQ})]\cdot 3H_2O$	447[b]	Diam.	4
14	$[(HL^2)UO_2(Gly)]\cdot 0.5H_2O$	449[b]	Diam.	4
15	$[(L^2)UO_2(Sal)]\cdot H_2O$	436[b]	Diam.	10
16	$[(HL^2)UO_2(Bac)]\cdot H_2O$	443[b]	Diam.	13

[a] Solutions in DMF (10^{-3} M), values of ε_{max} are in parentheses and multiplied by 10^{-4} (mol^{-1} dm^3 cm^{-1})

[b] Nujol mull

spectra, powder XRD as well as magnetic susceptibility and conductivity measurements. The prepared complexes are stable at room temperature, non-hygroscopic, and insoluble in water and most common organic solvents. The melting points of the complexes are above 300 °C.

The following representative equations illustrate the formation of some of the prepared complexes:

$$H_2L^1 + VOSO_4 \cdot H_2O + 3H_2O \rightarrow \left[(L^1)VO\right] \cdot 4H_2O\,(\mathbf{1}) + H_2SO_4$$

$$H_2L^1 + UO_2(OAc)_2 \cdot 2H_2O + 2CH_3OH \rightarrow \left[(L^1)UO_2\right] \cdot 2CH_3OH\,(\mathbf{4}) + 2AcOH + 2H_2O$$

$$H_2L^1 + UO_2(OAc)_2 \cdot 2H_2O + 8\text{ - }HQ \rightarrow \left[(L^1)UO_2(8\text{ - }HQ)\right]\,(\mathbf{5}) + 2AcOH + 2H_2O$$

$$H_2L^2 + Ce(NO_3)_3 \cdot 6H_2O + 2LiOH \cdot H_2O \rightarrow \left[(L^2)Ce(NO_3)\right] \cdot 2.5H_2O\,(\mathbf{10}) + 2LiNO_3 + 7.5H_2O$$

$$H_2L^2 + Ce(NO_3)_3 \cdot 6H_2O + 2LiOH \cdot H_2O \rightarrow \left[(L^2)Ce(NO_3)\right] \cdot 2.5H_2O\,(\mathbf{10}) + 2LiNO_3 + 7.5H_2O$$

$$H_2L^2 + UO_2(OAc)_2 \cdot 2H_2O + Gly \rightarrow \left[(HL^2)UO_2(Gly)\right] \cdot 0.5H_2O\,(\mathbf{14}) + 2AcOH + 1.5H_2O$$

IR spectra

The IR spectra of the complexes were compared with those of the free ligands to determine the coordinating sites that may be involved in chelation. There are some guide bands in the spectra of the ligands, which are of good help for achieving this goal. These bands are bands assigned to ν(C=O), ν(C=N), and ν(C–O)phenolic. The strong bands assigned to ν(C=O) and ν(C=N) in the free ligands were shifted to lower frequencies in the complexes, indicating the coordination of these groups to metal ions. On the other hand, the band assigned to ν(C–O)phenolic was shifted to higher frequencies in the complexes, suggesting the participation of the phenolic –OH group in chelation [41]. Also, all complexes showed a broad band in the range 3,385–3,576 cm^{-1} which can be assigned to the stretching frequency of the ν(OH) of the phenolic –OH group of the ligands, uncoordinated water and/or alcohol molecules associated with the complexes which are confirmed by elemental and thermal analyses. In complexes **3**, **10**, and **11** the new bands observed in the ranges 1,360–1,384 and 1,058–1,203 cm^{-1} may be assigned to the monodentate NO_3^- group [41, 42]. On the other hand, complex **2** showed a new band at 1,423 cm^{-1} that may be assigned to ionic NO_3^- group [43, 44]. The mixed 8-hydroxyquinoline complexes **5** and **13** showed new bands at 1,499 and 1,497 cm^{-1}, respectively, which may be assigned to the coordinated C=N group of the 8-hydroxyquinoline moiety [43, 45, 46]. The mixed glycine complexes **6** and **14** showed new bands in the ranges 1,510–1,516 and 1,300–1,362 cm^{-1} that may be assigned to $\nu_{as}(COO^-)$ and $\nu_s(COO^-)$, respectively, of the amino acid [13, 47]. The higher difference between asymmetric and symmetric vibrations suggests monodentate coordination of the carboxyl group of glycine with the metal ion [48, 49]. The characteristic band of the ν(V=O) is observed in the IR spectra of the oxovanadium(IV) complexes **1** and **9** at 954 and 980 cm^{-1}, respectively [41, 50, 51]. Also, the dioxouranium(VI) complexes **4**–**8** and **12**–**16** showed strong absorption bands in the range 885–903 cm^{-1} which can be assigned to the antisymmetric ν_3(O=U=O) vibration [52–54]. The values of ν(V=O) and ν(O=U=O) are used to calculate the force constant (F) of (V=O) and (O=U=O) by the method of McGlynn and Smith [55]: $(\nu)^2 = (1{,}307)^2 (F_{M-O})/14.103$. The calculated force constant values for the oxovanadium(IV) and dioxouranium(VI) complexes are found to be in the ranges 7.514–7.929 and 6.466–6.732 mdyn/Å, respectively. The M–O distance is also calculated by substitution in Jones relation [56]: $R_{M-O} = 1.08(F_{M-O})^{-1/3} + 1.17$. The values of R_{M-O} for oxovanadium(IV) and dioxouranium(VI) complexes are found to be in the ranges 1.712–1.721 and 1.742–1.750 Å, respectively. The calculated F_{M-O} and R_{M-O} values fall in the usual range for the oxovanadium(IV) and dioxouranium(VI) complexes [57–59]. Finally, the new bands in the ranges 506–595 and 423–499 cm^{-1} can be assigned to the stretching frequencies of ν(M–O) and ν(M–N), respectively [41, 43].

Conductivity measurements

The molar conductance values of the complexes in DMF (10^{-3} M solutions) were measured at room temperature and the results are listed in Table 1. The values showed that all complexes have non-electrolytic nature except complex **2** which gave molar conductance value = 71 Ω^{-1} cm^2 mol^{-1}, suggesting its 1:1 electrolytic nature. This is consistent with the infrared data that showed the presence of an ionic nitrate group. In case of complexes **3** and **11**, the relatively high values of the molar conductance data may be due to the partial dissociation in their DMF solutions; however, they did not reach the previously reported values for 1:1 electrolytes in DMF solutions (~70–110 Ω^{-1} cm^2 mol^{-1}) [60].

Electronic spectra and magnetic moment measurements

The electronic spectra of the metal complexes (Table 1) were carried out as DMF solutions and/or Nujol mulls where some metal complexes were sparingly soluble in most common solvents. Comparison of the spectra of the

free ligands with their complexes showed the persistence of the ligand bands in all complexes. The bands of the free ligands were slightly shifted to blue or red regions of the spectrum in all complexes. Also, new bands were observed in the spectra of the complexes which are listed in Table 1.

The electronic spectra of the oxovanadium(IV) complexes **1** and **9** showed new bands in the range 541–548 nm that may be assigned to the $^2B_2 \rightarrow {}^2B_1$ (ν_2) transition in an octahedral geometry [61, 62]. In addition, the V=O stretching frequencies for the complexes appeared in the range 954–980 cm^{-1} supporting the octahedral geometry of the complexes [63, 64]. The magnetic moment values (Table 1) of the oxovanadium(IV) complexes of H_2L^1 and H_2L^2 ligands are 1.42 and 1.00 BM, respectively. These values are lower than reported (1.74–2.10 BM) and refer to the interaction of the oxovanadium(IV) ion with neighboring central ions [61].

The electronic spectra of the Ce(III) complexes **2** and **10** and Th(IV) complexes **3** and **11** showed new absorption bands in the ranges 502–521 and 452–460 nm, respectively, which may be caused by charge transfer [52, 65–67]. The magnetic moment values of the Ce(III) complexes **2** and **10** are in the range 2.00–2.06 BM, which are close to the normal experimental range of 2.14–2.46 BM [68, 69].

The electronic spectra of the dioxouranium(VI) complexes **4–8** and **12–16** showed new absorption bands in the range 436–510 nm, which may be attributed to an electronic transition from the apical oxygen atoms to f-orbitals of the uranium(VI) ion or due to a charge transfer transition from the ligand to uranium(VI) ion [41, 52, 65, 70].

^1H and ^{13}C NMR spectra

The ^1H NMR spectra of the complexes **3–5** and **11–16** were recorded in DMSO-d_6 with reference to TMS. Inspection of these data reveals the following. (1) The disappearance of signals assigned to OH groups in complexes **3–5**, **11–13**, and **15** referring to their involvement in coordinating with metal ion after deprotonation [50]. However, in case of complexes **14** and **16**, the signal appeared but with reduced integration (1H), indicating that the ligand acts as a monobasic ligand [65]. (2) The signals observed in the ranges 9.20–13.65, 7.09–10.46, and 7.08–9.97 ppm may be assigned to NH, HC=N, and aromatic protons, respectively. In case of complexes **5**, **13**, **14**, and **15** new signals observed in the range 10.75–11.08 ppm (complexes **5** and **13**), at 10.04 (complex **14**), and 11.0 ppm (complex **15**) that may be assigned to the coordinated OH groups of the 8-hydroxyquinoline [71] and salicylaldehyde and NH_2 group of glycine moieties [15] supporting the formation of ternary complexes. Finally, the absence of OH protons (hydrated H_2O) may be due to their replacement by DMSO-d_6 molecules [50, 65].

The ^{13}C NMR spectra of the complexes **4**, **5**, **12**, and **13** were recorded in DMSO-d_6 with reference to TMS. The signals observed at 174.89 and 158.5 ppm in complex **4**, 175 and 155.02 ppm in complex **5**, 173.55 and 168.82 ppm in complex **12**, and 168.48 and 167.45 ppm in complex **13** can be assigned to C=O and C=N, respectively. The shift observed in positions of these signals, as compared to ligands, indicates the participation of the (C=O) and (C=N) groups in chelation. Aromatic carbon atoms were detected at appropriate shifts for all complexes. Complexes **5** and **13** showed new signals that confirmed the participation of 8-hydroxyquinoline moiety in chelation [72, 73], which is consistent with ^1H NMR and IR spectral data. Unfortunately, the solubility of the complexes **3**, **11**, and **14–16** was not sufficient for ^{13}C NMR measurements.

ESR spectra

The X-band ESR spectrum of a powdered sample of $[(L^1)VO]\cdot 4H_2O$ (**1**) at room temperature (Fig. S3 (A), Supplementary material) showed a broad band centered on $g = 1.97$, without resolved hyperfine structure. In particular, the hyperfine coupling with the nearby ^{51}V ($I = 7/2$) nucleus is not observed. The absence of vanadium hyperfine coupling is common in solid state samples [74] and is attributed to the simultaneous flipping of neighboring electron spins [75, 76] or due to strong exchange interactions, which average out the interaction with the nuclei.

On the other hand, the ESR spectrum of $[(L^2)VO]\cdot 3H_2O$ (**9**) at room temperature (Fig. S3 (B), Supplementary material) exhibited an eight-line pattern corresponding to the usual parallel and perpendicular components of g- and hyperfine (hf) A-tensors. The calculated $g_\parallel$ and $g_\perp$ are 1.97 and 2.02, respectively. The $A_\parallel$ and $A_\perp$ values are 162×10^{-4} and 72×10^{-4} cm^{-1}, respectively. These ESR parameters and energy of *d–d* transition were used to evaluate the molecular orbital coefficients α^2 and β^2 for the complex using the following equations [77]

$$\alpha^2 = \frac{(2.0027 - g_\parallel)E_{d-d}}{8\lambda\beta^2}$$

$$\beta^2 = \frac{7}{6}\left[\left(\frac{-A_\parallel}{P}\right) + \left(\frac{A_\perp}{P}\right) + \left(g_\parallel - \frac{5}{14g_\perp}\right) - \frac{9}{14g_e}\right]$$

where $P = 128 \times 10^{-4}$ cm^{-1}, $\lambda = 135$ cm^{-1}, and E is the energy of the d–d transition. The calculated values were $\alpha^2 = 0.62$ and $\beta^2 = 0.90$ which agree well with those reported for octahedral configuration around the oxovanadium(IV) ion [61]. The lower value of α^2 compared to β^2 indicates that the in-plane σ-bonding is more covalent than the in-plane π-bonding [78, 79].

Thermal analysis

In the current study, the aim of thermal gravimetric analyses is to obtain information concerning the thermal stability of the prepared compounds and decide whether the water and solvent molecules are in the inner or outer coordination sphere of the central metal ion [80]. The H_2L^1 and H_2L^2 ligands are stable up to 250 and 192 °C, respectively. Greater stability of the ligands compared with their complexes suggests a powerful intramolecular H-bonding in the ligands [81, 82]. Complexes **1**, **6**, **8**, **14**, **15**, and **16** were taken as representative examples for thermal analysis. The results of thermal analysis of the complexes (Table 2) are in good agreement with the theoretical formulae as suggested from elemental analyses. The first stage of decomposition of the complexes extends up to 135 °C, corresponding to the loss of non-coordinated or solvated water or methanol molecules during an exothermic process in most cases. The second stage of decomposition extends up to 333 °C corresponding to the loss of the secondary ligand (glycine or benzoylacetone) molecules during an exothermic process in most cases.

Mass spectra

The mass spectra of the complexes $[(L^1)VO]\cdot 4H_2O$ (**1**), $[(L^1)UO_2(8\text{-HQ})]$ (**5**), and $[(L^2)Th(NO_3)_2]\cdot 4H_2O$ (**11**) as representative complexes are depicted in Fig. S2 (Supplementary material). Complex **5** showed the parent peak at $m/z = 801$ which compares very well with the formula weight of the complex (801.47). However, complexes **1** and **11** showed the parent peaks at $m/z = 453$ and 752, respectively, which compare very well with the calculated formula weights of the anhydrous complexes $[(L^1)VO]$ (453.29) and $[(L^2)Th(NO_3)_2]$ (752.52).

Powder X-ray diffraction

Although single-crystal X-ray crystallographic investigation is the most precise source of information regarding the structure of a complex, the difficulty of obtaining crystalline complexes renders this method unsuitable for such a study. However, a variety of other techniques could be used with good effect for characterizing the metal complexes as X-ray powder diffraction. So, X-ray powder diffraction (XRD) measurements of the H_2L^1 ligand and complexes **4** and **5** were performed as representative examples. The diffractograms obtained of the ligand and complexes have been given in Fig. 2 and the observed diffraction data, i.e., interplanar spacing d (Å), relative intensities (I/I^0), and 2θ observed of the samples have been given in Table S2 (Supplementary material). The mean crystallite size calculations were performed using Debye–Sherrer's equation [83]

$$D = K\lambda/(\beta\cos\theta),$$

where D is the particle size in nm of the crystal grain, K is a constant (0.94 for Cu grid), λ is the wavelength of target used, β is the full width at half-maximum reflection height in terms of radian, and θ is the Bragg diffraction angle at peak position in degree. The values obtained for crystallite size (Table 3) indicated that the particles were nano-sized. The CRYSFIRE computer program [84] was used to calculate the lattice parameters. The lattice parameters of the H_2L^1 ligand are $a = 6.944$ Å, $b = 9.748$ Å, $c = 12.52$ Å, $\alpha = 131.85°$, $\beta = 79.31°$, and $\gamma = 83.71°$. The crystal system and space group of the ligand are triclinic and P-1, respectively. The lattice parameters of complex **4** are $a = 7.706$ Å, $b = 11.479$ Å, $c = 18.613$ Å, $\alpha = 58.84°$, $\beta = 67.68°$, and $\gamma = 98.70°$. The analysis indicates that complex **4** has triclinic structure with space group $P1$.

Table 2 Thermal analyses data (TG-DSC) of some metal complexes of H_2L^1 and H_2L^2 ligands

Complex	Temperature range/°C	% wt. loss found (calc.)	DSC peak/°C		ΔH/J g^{-1}	Lost fragment
			Exo	Endo		
$[(L^1)VO]\cdot 4H_2O$ (**1**)	30–103	13.66 (13.71)	81		−6.73	4 H_2O (hyd.)
$[(HL^1)UO_2(Gly)]\cdot 0.5MeOH$ (**6**)	25–95	2.15 (2.14)	73		−8.22	0.5 MeOH (solv.)
$[(HL^1)UO_2(Bac)]\cdot MeOH$ (**8**)	38–100	3.94 (3.76)	54		−2.5	1 MeOH (solv.)
	100–328	18.88 (19.05)		277	1.23	1 Bac
$[(HL^2)UO_2(Gly)]\cdot 0.5H_2O$ (**14**)	25–127	1.28 (1.20)		82	11.21	0.5 H_2O (hyd.)
	127–321	10.22 (9.99)	161		−1.78	1 Gly
$[(L^2)UO_2(Sal)]\cdot H_2O$ (**15**)	38–112	2.28 (2.23)		67	0.42	1 H_2O (hyd.)
	112–392	15.36 (15.13)	282		−22.98	1 Sal
$[(HL^2)UO_2(Bac)]\cdot H_2O$ (**16**)	39–135	2.35 (2.13)	112		−1.59	1 H_2O (hyd.)
	135–333	19.32 (19.13)	202		−110	1 Bac

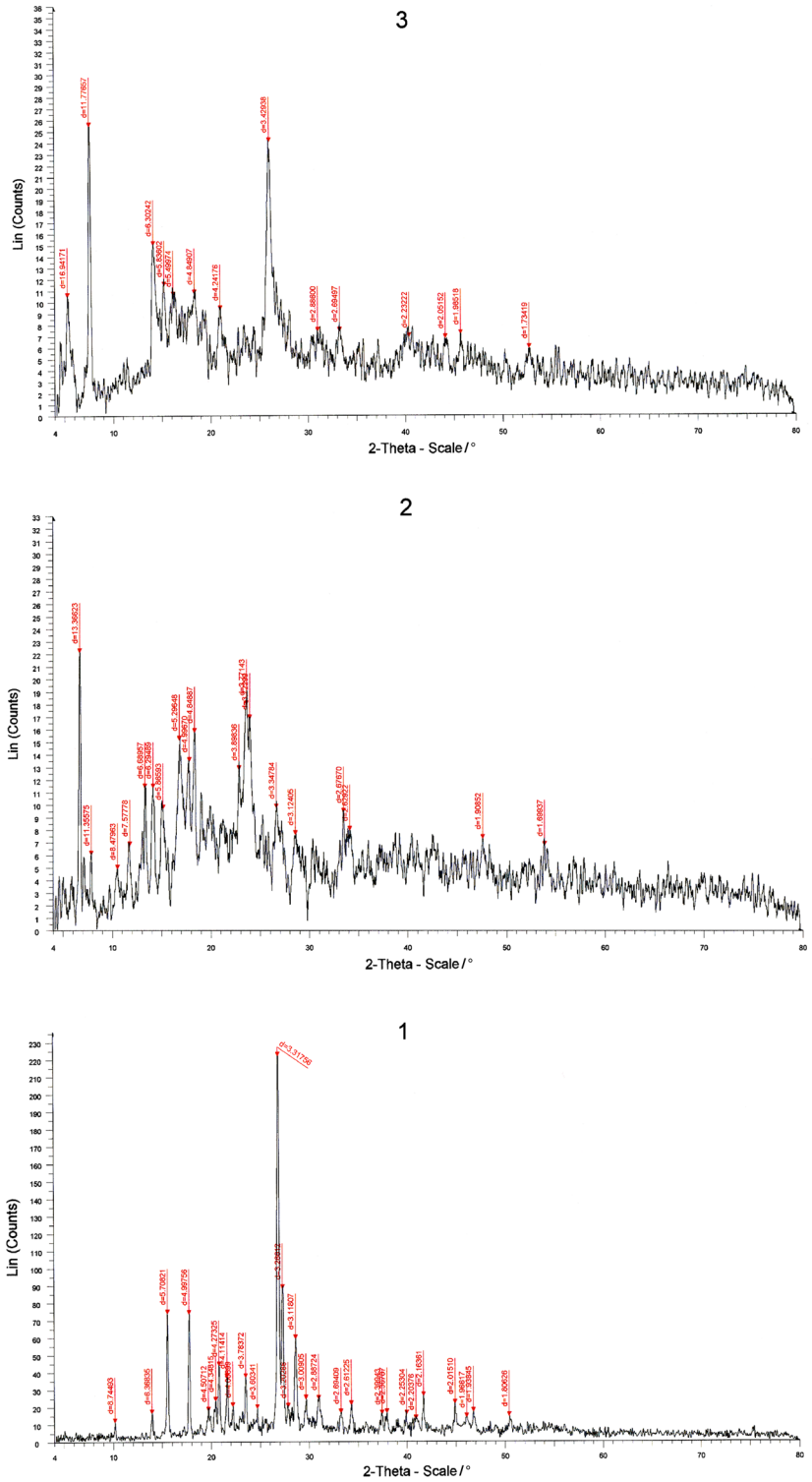

Fig. 2 X-ray diffraction pattern of (*1*) H_2L^1 ligand, (*2*) $[(L^1)UO_2]\cdot 2MeOH$, complex **4** and (*3*) $[(L^1)UO_2(8\text{-HQ})]$, complex **5**

Finally, the lattice parameters of complex **5** are $a = 13.483$ Å, $b = 16.972$ Å, $c = 6.785$ Å, $\alpha = 90°$, $\beta = 118.88°$, and $\gamma = 90°$. The crystal system and space group of the complex are monoclinic and *P2/m*, respectively.

Finally, from the interpretation of elemental and thermal analyses and spectral data (infrared, electronic, mass, ^{1}H and ^{13}C NMR, and ESR) as well as magnetic susceptibility measurements at room temperature and conductivity measurements, it is possible to draw up the tentative

Table 3 Particle sizes of H_2L^1 ligand and its dioxouranium(VI) complexes **4** and **5**

	2θ	d/Å	FWHM; β	Crystallite size/nm
H_2L^1	26.852	3.318	2.457×10^{-3}	60.6
$[(L^1)UO_2]\cdot 2MeOH$ (**4**)	6.608	13.366	1.822×10^{-3}	79.6
$[(L^1)UO_2(8\text{-HQ})]$ (**5**)	7.501	11.777	2.738×10^{-3}	53

structures of the metal complexes. Figures 3, 4, 5, and 6 represent the proposed structures of the metal complexes.

Antimicrobial activity

The antimicrobial activity of the ligands and their metal complexes was investigated against the sensitive organisms: *Staphylococcus aureus* (ATCC 25923) and *Bacillus subtilis* (ATCC 6635) as Gram-positive bacteria, *Escherichia coli* (ATCC 25922) and *Salmonella typhimurium* (ATCC 14028) as Gram-negative bacteria, yeast *Candida albicans* (ATCC 10231), and fungus *Aspergillus fumigatus*. The results are listed in Table 4. Inspection of the data given in Table 4 reveals that the ligands and their metal complexes (except cerium(III) and thorium(IV) complexes) are biologically active toward the tested organisms. It is clear that H_2L^2 ligand is more active than H_2L^1 ligand toward all organisms. Also, the activity of the ligands is enhanced by chelation. This enhancement in activity due to chelation can be explained on the basis of chelation theory [85]. Chelation reduces the polarity of the metal ion considerably, mainly because of the partial sharing of its positive charge with donor groups and the possible π-electron delocalization over the whole chelate ring. Chelation not only reduces the polarity of metal ion, but also increases the lipophilic character of the chelate. As a result of this, interaction between metal ion and the cell walls is favored resulting in interference with normal cell processes. If the geometry and charge distribution around the molecule are incompatible with the geometry and charge distribution around the pores of the bacterial cell wall, penetration through the wall by the toxic agent cannot take place, preventing toxic reaction within the pores [86].

The minimum inhibitory concentration (MIC) was determined for the synthesized compounds and the results are listed in Table 5. H_2L^2 is more active than H_2L^1 toward all organisms. The complexes showed enhanced activity than the ligands. Against *Staphylococcus aureus*, complex **5** showed a promising activity (MIC = 2 μg/cm^3) while complex **9** showed an intermediate activity (MIC = 16 μg/cm^3). The other complexes showed lower activity (MIC = 60–70 μg/cm^3). Against *Bacillus subtilis*, complex **5** showed a higher activity (MIC = 4 μg/cm^3) while complexes **1**, **4**, **8**, and **9** showed an intermediate activity (MIC = 8–18 μg/cm^3). The other complexes showed lower activity (MIC = 36–42 μg/cm^3). Against *Salmonella typhimurium*, complexes **4**, **5**, and **13** showed an intermediate activity (MIC = 15–18 μg/cm^3) while complex **12** showed a lower activity (MIC = 66 μg/cm^3). Against *Escherichia coli*, complex **5** showed a promising higher activity (MIC = 6 μg/cm^3) while complexes **8**, **9**, and **12–14** showed an intermediate activity (MIC = 43–45 μg/cm^3) and complex **4** showed a lower activity (MIC = 68 μg/cm^3). Against *Candida albicans*, complex **5** showed a promising higher activity (MIC = 2 μg/cm^3) while complexes **1** and **9** showed an intermediate activity (MIC = 6–7 μg/cm^3). The other complexes showed lower activity (MIC = 26–31 μg/cm^3). Finally, against *Aspergillus fumigatus*, complex **5** showed a

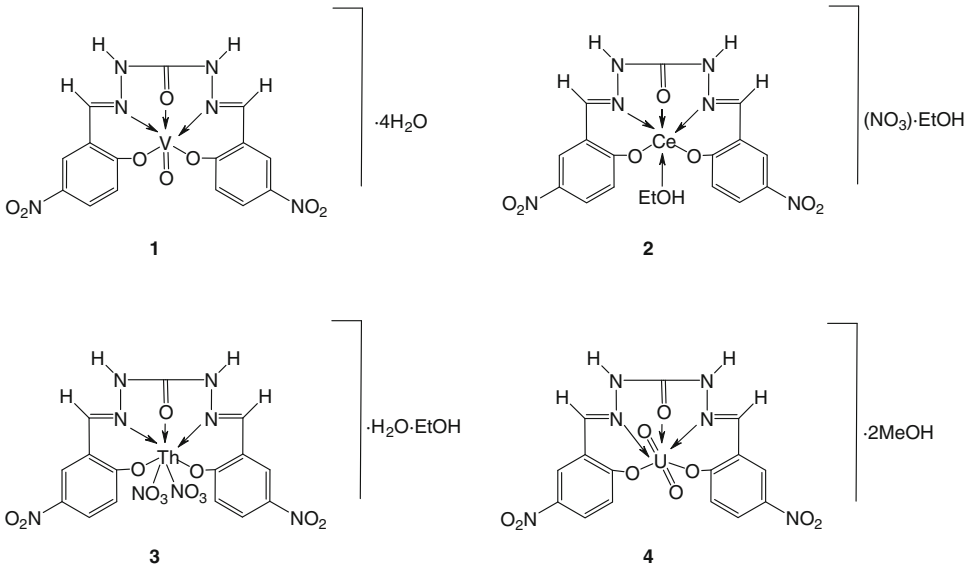

Fig. 3 Representative structures of oxovanadium(IV), Ce(III), Th(IV), and dioxouranium(VI) complexes of the carbohydrazone ligand H_2L^1

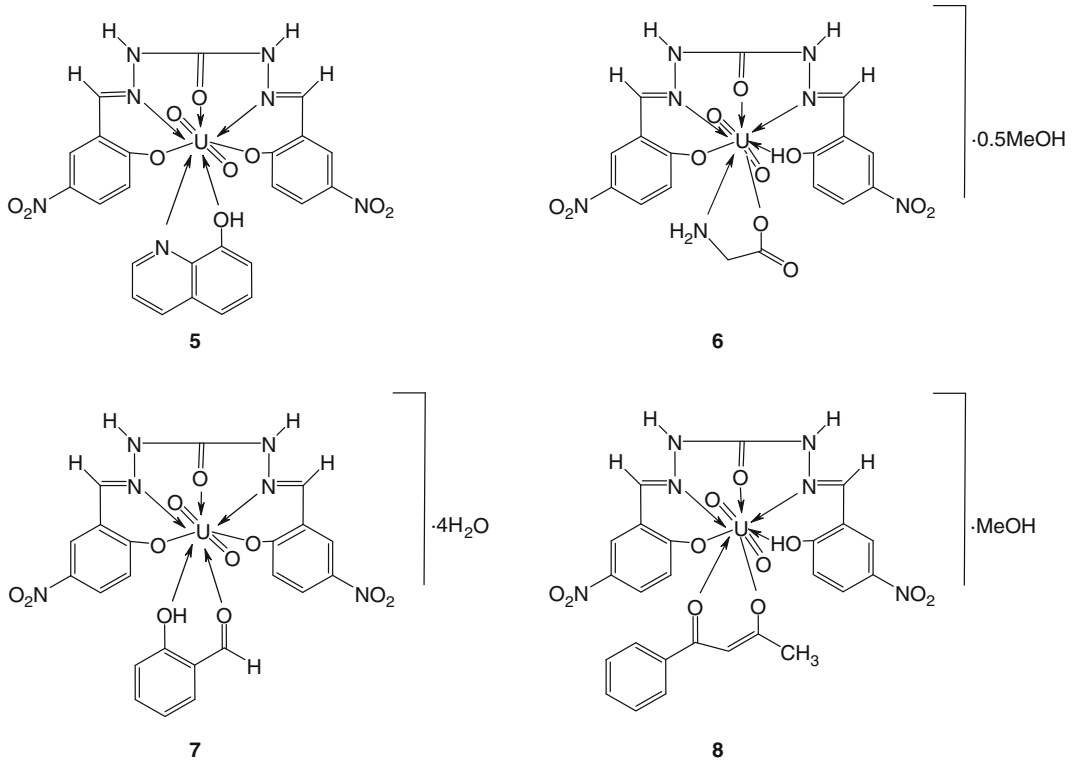

Fig. 4 Representative structures of ternary dioxouranium(VI) complexes of the carbohydrazone ligand H_2L^1

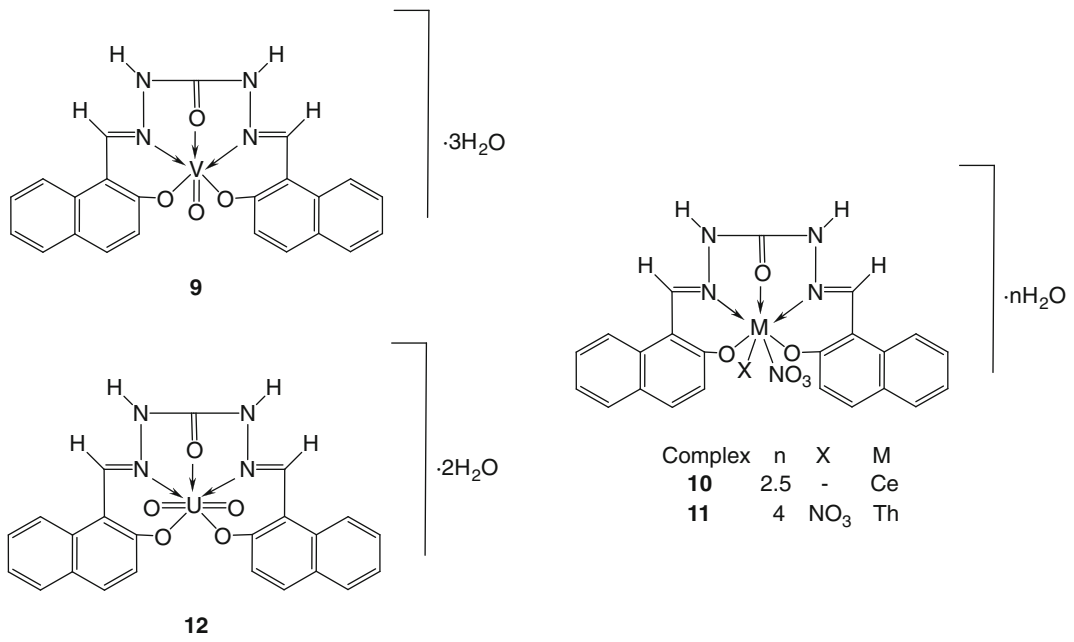

Fig. 5 Representative structures of oxovanadium(IV), Ce(III), Th(IV), and dioxouranium(VI) complexes of the carbohydrazone ligand H_2L^2

promising higher activity (MIC = 1 μg/cm^3) while complexes **1** and **13** showed an intermediate activity (MIC = 8 μg/cm^3). The other complexes (**4** and **12**) showed lower activity (MIC = 36–38 μg/cm^3).

Finally, the dioxouranium(VI) complex **5** seems to be promising as it showed antimicrobial activity and MIC values that are comparable to (and sometimes higher than) those of chloramphenicol, cephalothin, and cycloheximide

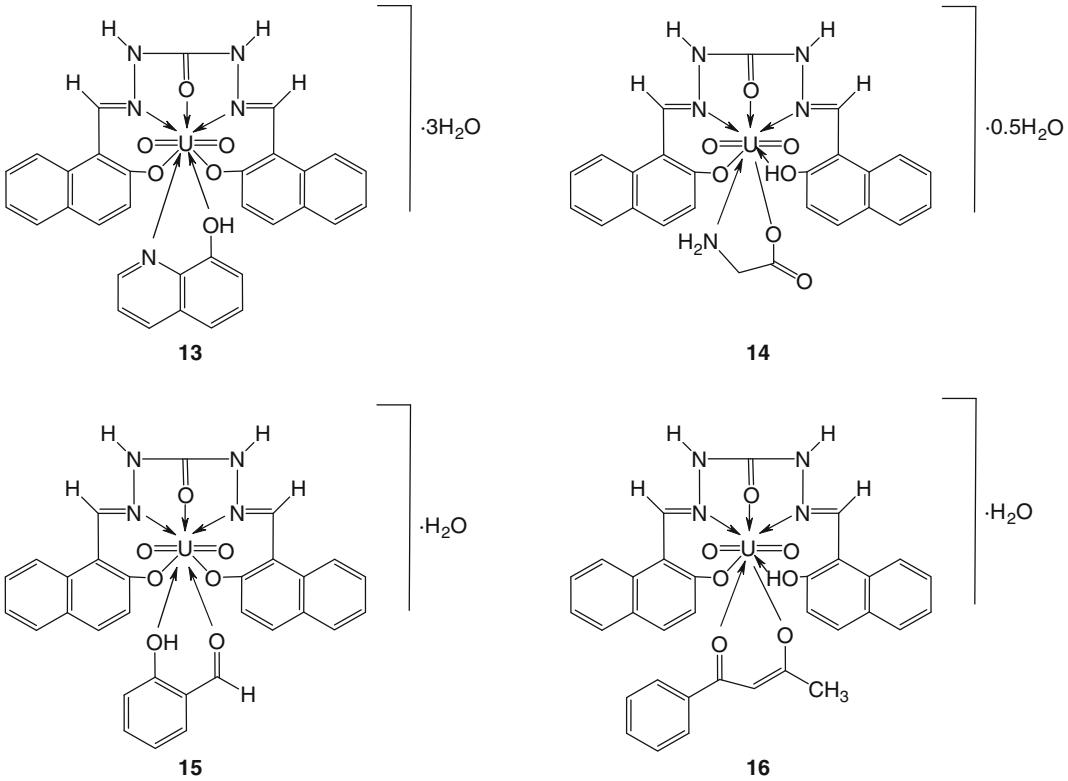

Fig. 6 Representative structures of ternary dioxouranium(VI) complexes of the carbohydrazone ligand H_2L^2

and thus can be further explored as specific antimicrobial drugs.

DNA binding affinity of oxovanadium(IV) complexes

As one of the trace bioelements existing in the human body, vanadium complexes have been found to present numerous biological and pharmaceutical applications. This bioelement takes part in various DNA maintenance reactions and thereby prevents genomic instability which otherwise leads to cancer. In the current study, the DNA binding properties of the oxovanadium(IV) complexes were investigated by electronic absorption spectroscopy and viscosity measurements.

Electronic spectral studies

Electronic absorption spectroscopy has been widely employed to determine the binding ability of metal complexes with DNA [87–90]. The binding ability of the synthesized oxovanadium(IV) complexes $[(L^1)VO]\cdot 4H_2O$ (**1**) and $[(L^2)VO]\cdot 3H_2O$ (**9**) with HS-DNA was investigated by measuring the spectral changes of their electronic spectra during the interaction with DNA. Complex binding with DNA through intercalation usually results in hypochromism and bathochromism, due to intercalative mode involving a strong stacking interaction between an aromatic chromophore of the bound ligand and the base pairs of DNA [91, 92]. Therefore, to obtain the evidence for the binding mode of compounds to DNA, spectroscopic titrations of compound solutions with DNA have been performed. Absorption titration experiments of oxovanadium(IV) complexes in buffer were performed using a fixed concentration of oxovanadium(IV) complex to which increments of the DNA stock solution were added. The absorption spectra of complex **9** in the absence and presence of DNA are given in Fig. 7. The binding of oxovanadium(IV) complexes **1** and **9** to duplexes DNA led to decrease in the absorption intensities (hypochromism) with a small amount of red shifts in the UV–Vis absorption spectra (bathochromism) where in the presence of DNA, the absorption bands at about 221 for complexes **1** and **9** exhibited hypochromism of 32.7 and 33.8 %, respectively (Table 6). The extent of hypochromism is consistent with intercalative interaction [93]. After intercalating the base pairs of DNA, the π* orbital of the intercalated ligand can couple with the π orbital of the base pairs, thus decreasing the π–π* transition energy and resulting in the bathochromism [94]. On the other hand, the coupling π* orbital is partially filled by electrons, thus decreasing the transition

probabilities and concomitantly resulting in hypochromism. To compare quantitatively the affinity of the two complexes toward DNA, the binding constants K_b of the two complexes to HS-DNA were determined by monitoring the changes of absorbance at 221 nm for the complexes, with increasing concentration of DNA. The appreciable decrease in absorption intensity and red shift of the λ_{max} band suggest that the complexes bind to DNA strongly [87–90, 95]. From the absorption titration data, the binding constant (K_b) was determined using the following equation [96]:

$$\frac{c}{\Delta\varepsilon_a} = \frac{c}{\Delta\varepsilon} + \frac{1}{\Delta\varepsilon K_b}$$

where c = [DNA], $\Delta\varepsilon_a = |\varepsilon_a - \varepsilon_f|$, and $\Delta\varepsilon = |\varepsilon_b - \varepsilon_f|$ (ε_a, ε_f, and ε_b are extinction coefficient observed (A_{obs}/[complex]), extinction coefficient of the free complex, and extinction coefficient of the complex fully bound to DNA, respectively).

The ratio of slope to intercept in the plot of [DNA]/$\Delta\varepsilon_a$ vs. [DNA] (Fig. 7, insert) gave the value of K_b. The binding constants (K_b) of complexes **1** and **9** are calculated as 2.55×10^4 and 3×10^4 M^{-1}, respectively. The obtained K_b values are consistent with those of DNA-intercalative oxovanadium(IV) complexes [97, 98] and revealed that complex **9** shows a stronger binding ability toward DNA which may be due to the presence of an appending aromatic moiety in H_2L^2 ligand and thus the larger binding affinity of the corresponding complex **9** in comparison with complex **1** incorporating H_2L^1 ligand [35, 99–101].

Viscosity measurements

Optical or photophysical probes generally provide necessary, but not sufficient clues to support an intercalative binding mode. To further clarify the interaction mode between the oxovanadium(IV) complexes and HS-DNA, viscosity measurement was carried out. Viscosity measurement, which is sensitive to changes in the length of DNA, is regarded as the least ambiguous and most critical means of evaluating the binding mode of complexes with DNA in solution in the absence of crystallographic structural data [102] and can provide strong evidence for intercalative binding mode [103, 104]. In classical intercalation, the DNA helix lengthens as the base pairs are separated to accommodate the bound compound, leading to increased DNA viscosity, whereas in groove binding and electrostatic mode the length of the helix is unchanged resulting in no apparent alteration in DNA viscosity. In contrast, a partial, non-classical intercalation causes a bend in DNA helix, reducing its effective length and thereby its viscosity [105]. The effect of the oxovanadium(IV) complexes on the viscosity of HS-DNA is illustrated in Fig. 8, which indicates that the relative viscosity of HS-DNA increases steadily with increasing the concentration of the oxovanadium(IV) complex. This verifies that the complexes bind to DNA in the mode of intercalation [103, 104] which is consistent with the forgoing spectral study. Thus, based on spectroscopic study together with viscosity measurements, we can conclude that oxovanadium(IV) complexes interact with the DNA through an intercalation mode.

Conclusion

The condensation reaction of carbohydrazide with 2-hydroxy-5-nitrobenzaldehyde and 2-hydroxy-1-naphthaldehyde, respectively, stoichiometrically in the molar ratio 1:2 (carbohydrazide:aldehyde) afforded the pentadentate N_2O_3 ligands. Reactions of the ligands with oxovanadium(IV), cerium(III), thorium(IV), and dioxouranium(VI) ions yielded binary complexes. In the presence of secondary ligands, reactions of the ligands with the dioxouranium(VI) ion yielded ternary complexes. The ligands and their metal complexes were identified by elemental and thermal analyses, IR, ^1H and ^{13}C NMR, electronic, ESR, mass spectra, and powder XRD as well as magnetic susceptibility and conductivity measurements. The results showed that the ligands act as dibasic pentadentate except complexes **6**, **8**, **14**, and **16** in which the ligands act as monobasic pentadentate ligands. Based on XRD data it was found that the H_2L^1 ligand and complex **4** have triclinic system while complex **5** has monoclinic system with different unit cell parameters. The ligands and some complexes were found to be biologically active. The DNA binding properties of the oxovanadium(IV) complexes were investigated by electronic absorption and viscosity measurements. The results showed that these complexes bind to DNA via an intercalation binding mode.

Experimental

Microanalyses of carbon, hydrogen, and nitrogen were carried out on Vario El Elementar apparatus at the National Research Centre, Dokki, Giza, Egypt. Melting points of the metal complexes were determined using a Stuart melting point instrument. Analyses of the metals followed the dissolution of the solid complex in concentrated HNO_3, neutralizing the diluted aqueous solutions with ammonia, and titrating the metal solutions with EDTA. IR spectra were recorded using KBr discs on FT IR Nicolet IS10 spectrometer. Electronic spectra were recorded as solutions in DMF or Nujol mulls on a Jasco UV–Vis

spectrophotometer model V-550 UV–Vis. ^{1}H and ^{13}C NMR spectra were recorded at room temperature using a Bruker WP 200 SY spectrometer. Dimethylsulfoxide (DMSO-d_6) was used as a solvent and tetramethylsilane (TMS) as an internal reference. The chemical shifts (δ) are given downfield relative to TMS. D_2O was added to test for the deutration of the samples. ESR spectra of the complexes were recorded at an Elexsys, E500, Bruker company. The magnetic field was calibrated with a 2,2′-diphenyl-1-picrylhydrazyl (DPPH) sample purchased from Aldrich. Mass spectra were recorded at 70 eV on a Gas chromatographic GCMSqp 1000 ex Shimadzu instrument. The magnetic susceptibility measurements were carried out at room temperature using a magnetic susceptibility balance of the type Johnson Matthey, Alfa product, Model No. (MKI). Effective magnetic moments were calculated from the expression $\mu_{\text{eff.}} = 2.828\ (\chi_M\ T)^{1/2}$ BM, where χ_M is the molar susceptibility corrected using Pascal's constants for the diamagnetism of all atoms in the compounds [106]. Molar conductivities of 10^{-3} M solutions of the solid complexes in DMF were measured on a Corning conductivity meter NY 14831 model 441. TG-DSC measurements were carried out on a Shimadzu-50 instrument. Powder X-ray diffraction (XRD) measurements were performed at ambient temperature using a D8 Advance X-ray diffractometer (Bruker AXS, Germany). The diffraction pattern was recorded for 2θ from 4° to 80° at room temperature using CuKα monochromated radiation ($\lambda = 1.54060$ Å) with the following measurement conditions: tube voltage of 40 kV, tube current of 40 mA, step scan mode with a step size of $2\theta = 0.02°$.

$VOSO_4{\cdot}H_2O$, $Ce(NO_3)_3{\cdot}6H_2O$, $Th(NO_3)_4{\cdot}5H_2O$, $UO_2(OAc)_2{\cdot}2H_2O$, $LiOH{\cdot}H_2O$, carbohydrazide, 2-hydroxy-5-nitrobenzaldehyde, 2-hydroxy-1-naphthaldehyde, 8-hydroxyquinoline, glycine, salicylaldehyde, and benzoylacetone were purchased from Merck or BDH. Herring sperm DNA (HS-DNA) (Mallinckrodt) and tris(hydroxymethyl)-aminomethane–HCl (Tris–HCl) were used as received. Organic solvents [ethanol, absolute ethanol, methanol, diethylether, dimethylformamide (DMF), and dimethylsulfoxide (DMSO)] were reagent-grade chemicals and were used without further purification.

Synthesis of the ligands H_2L^1 and H_2L^2

The carbohydrazone ligands H_2L^1 and H_2L^2 were synthesized by adding carbohydrazide (5 mmol) in 30 cm^3 absolute ethanol to 2-hydroxy-5-nitrobenzaldehyde or 2-hydroxy-1-naphthaldehyde (10 mmol) dissolved in 30 cm^3 hot absolute ethanol. The reaction mixture was heated to reflux for 6 h. The obtained products were filtered off and washed with a few amounts of ethanol then diethylether and finally air-dried. The ligands were kept in a desiccator until used.

2,2′-[Carbonylbis(hydrazin-2-yl-1-ylidenemethylidyne)]-bis(4-nitrophenol) (H_2L^1, $C_{15}H_{12}N_6O_7$)
Yield 95 %; m.p.: >300 °C; IR (KBr): $\bar{\nu} = 3{,}431$ (OH), 3,275 (NH), 1,674 (C=O), 1,631 (C=N), 1,579 (C=C), 1,283 $(C–O)_{\text{phenolic}}$ cm^{-1}; ^{1}H NMR (300 MHz, DMSO-d_6): $\delta = 12.06$ (2H, OH), 11.24 (2H, NH), 8.14–8.72 (6H, Ar–H), 7.09, 7.12 (2H, HC=N) ppm; ^{13}C NMR (75 MHz, DMSO-d_6): $\delta = 163.72$ (C=O), 153.66 (C=N), 141.82 (C1), 127.77 (C4), 124.76 (C5), 122.55 (C3), 120 (C6), 118.50 (C2) ppm; UV–Vis (DMF, $c = 1 \times 10^{-3}$ mol dm^{-3}): $\lambda_{\max}$ (ε) = 279 (3,900), 296 (3,800), 352 (4,000), 384 (2,900), 448 (2,600) nm (mol^{-1} dm^3 cm^{-1}); MS (70 eV): $m/z = 388$ (M^+).

1,1′-[Carbonylbis(hydrazin-2-yl-1-ylidenemethylidyne)]-bis(naphthalen-2-ol) (H_2L^2, $C_{23}H_{18}N_4O_3$)
Yield 80 %; m.p.: 297 °C; IR (KBr): $\bar{\nu} = 3{,}323$ (OH), 3,212 (NH), 1,676 (C=O), 1,622 (C=N), 1,559 (C=C), 1,325 $(C–O)_{\text{phenolic}}$ cm^{-1}; ^{1}H NMR (300 MHz, DMSO-d_6): $\delta = 11.91$ (2H, OH), 11.07, 10.64 (2H, NH), 7.23–8.36 (12H, Ar–H), 9.22 (2H, HC=N) ppm; ^{13}C NMR (75 MHz, DMSO-d_6): $\delta = 156.70$ (C=O), 151.62 (C=N), 143.31 (C2), 141.77 (C8a), 131.53 (C4), 128.72 (C4a), 127.87 (C5), 127.54 (C7), 123.34 (C8), 121.51 (C6), 118.63 (C3), 109.39 (C1) ppm; UV–Vis (DMF, $c = 1 \times 10^{-3}$ mol dm^{-3}): $\lambda_{\max}$ (ε) = 270 (3,900), 292 (3,600), 350 (4,100), 385 (2,700), 420 (2,700) nm (mol^{-1} dm^3 cm^{-1}); MS (70 eV): $m/z = 398$ (M^+).

Synthesis of the metal complexes

An ethanolic solution of the metal salt (30 cm^3) was added gradually to the ethanolic solution of the ligands (40 cm^3) in the molar ratio 1:1 (M:L). The dioxouranium(VI) complexes were prepared in methanol as uranyl acetate is more soluble in this solvent. In case of oxovanadium(IV) and Th(IV) complexes, water was added to ensure the complete dissolution of metal salts. Th(IV) complexes of the two ligands and Ce(III) complex of H_2L^2 ligand were prepared successfully only in the presence of LiOH. The reaction mixture was heated to reflux for 6 h. The resulting precipitates were filtered off, washed with ethanol or methanol (in case of dioxouranium(VI) complexes) then diethylether, and finally air-dried. Most of the complexes are insoluble in common organic solvents but some of them are partially soluble in DMF and/or DMSO. The following detailed preparations are given as examples and the other complexes were obtained similarly.

Table 4 Antimicrobial activity of the carbohydrazone ligands H_2L^1 and H_2L^2 and their metal complexes

	Mean of zone diameter[a]/mm											
	Gram-positive bacteria				Gram-negative bacteria				Yeasts and fungi[b]			
	Staphylococcus aureus		*Bacillus subtilis*		*Salmonella typhimurium*		*Escherichia coli*		*Candida albicans*		*Aspergillus fumigatus*	
Sample conc/mg cm^{-3}: Compound	1	0.5	1	0.5	1	0.5	1	0.5	1	0.5	1	0.5
H_2L^1	6 L	5 L	5 L	4 L	7 L	5 L	8 L	6 L	6 L	4 L	7 L	5 L
$[(L^1)VO]\cdot 4H_2O$ (**1**)	–	–	12 I	9 I	–	–	–	–	13 I	8 L	20 I	15 I
$[(L^1)Ce(EtOH)]NO_3\cdot EtOH$ (**2**)	–	–	–	–	–	–	–	–	–	–	–	–
$[(L^1)Th(NO_3)_2]\cdot EtOH\cdot H_2O$ (**3**)	–	–	–	–	–	–	–	–	–	–	–	–
$[(L^1)UO_2]\cdot 2MeOH$ (**4**)	9 L	7 L	10 L	8 L	12 I	8 L	12 I	8 L	8 L	6 L	8 L	6 L
$[(L^1)UO_2(8\text{-HQ})]$ (**5**)	32 H	26 H	32 H	28 H	23 I	17 I	36 H	31 H	26 H	23 H	38 H	34 H
$[(HL^1)UO_2(Gly)]\cdot 0.5MeOH$ (**6**)	–	–	8 L	7 L	–	–	–	–	–	–	–	–
$[(L^1)UO_2(Sal)]\cdot 4H_2O$ (**7**)	–	–	10 L	8 L	–	–	–	–	8 L	7 L	–	–
$[(HL^1)UO_2(Bac)]\cdot MeOH$ (**8**)	–	–	13 I	9 I	–	–	15 I	10 I	11 L	7 L	–	–
H_2L^2	7 L	5 L	6 L	5 L	8 L	6 L	12 L	7 L	7 L	6 L	8 L	6 L
$[(L^2)VO]\cdot 3H_2O$ (**9**)	19 I	14 I	21 I	17 I	–	–	14 I	10 I	17 I	11 I	–	–
$[(L^2)Ce(NO_3)]\cdot 2.5H_2O$ (**10**)	–	–	–	–	–	–	–	–	–	–	–	–
$[(L^2)Th(NO_3)_2]\cdot 4H_2O$ (**11**)	–	–	–	–	–	–	–	–	–	–	–	–
$[(L^2)UO_2]\cdot 2H_2O$ (**12**)	8 L	6 L	8 L	7 L	9 L	7 L	13 I	8 L	8 L	7 L	9 L	7 L
$[(L^2)UO_2(8\text{-HQ})]\cdot 3H_2O$ (**13**)	10 L	8 L	9 L	7 L	12 I	8 L	13 I	8 L	8 L	7 L	20 I	16 I
$[(HL^2)UO_2(Gly)]\cdot 0.5H_2O$ (**14**)	8 L	7 L	8 L	7 L	–	–	20 I	15 I	–	–	–	–
$[(L^2)UO_2(Sal)]\cdot H_2O$ (**15**)	8 L	7 L	9 L	7 L	–	–	–	–	–	–	–	–
$[(HL^2)UO_2(Bac)]\cdot H_2O$ (**16**)	8 L	6 L	8 L	7 L	–	–	–	–	–	–	–	–
Control[c]	35	26	35	25	36	28	38	27	35	28	37	26

–, no effect

L, low activity = mean of zone diameter ≤1/3 of mean zone diameter of control

I, intermediate activity = mean of zone diameter ≤2/3 of mean zone diameter of control

H, high activity = mean of zone diameter >2/3 of mean zone diameter of control

[a] Calculated from three values

[b] Identified on the basis of routine cultural, morphological, and microscopical characteristics

[c] Chloramphenicol in the case of Gram-positive bacteria, cephalothin in the case of Gram-negative bacteria, and cycloheximide in the case of yeasts and fungi

[2,2′-[Carbonylbis(hydrazin-2-yl-1-ylidenemethylidyne)]-bis(4-nitrophenolato)]dioxouranium(VI)·2MeOH
(**4**, $C_{17}H_{18}N_6O_{11}U$)

Uranyl acetate dihydrate ($UO_2(OAc)_2\cdot 2H_2O$, 0.547 g, 1.29 mmol) in 30 cm^3 methanol was added gradually with constant stirring to the solution of 0.5 g of the ligand H_2L^1 (1.29 mmol) in 30 cm^3 methanol. The reaction mixture was heated to reflux for 6 h. An orange precipitate was formed, filtered off, and washed several times with small amounts of methanol then diethylether, and finally air-dried. The yield was 0.79 g (85 %). M.p.: >300 °C; IR (KBr): $\bar{\nu}$ = 3,437 (OH), 3,265 (NH), 1,647 (C=O), 1,602 (C=N), 1,566 (C=C), 1,309 $(C–O)_{phenolic}$, 595 (M–O), 491 (M–N), 898 (UO_2) cm^{-1}; ^1H NMR (300 MHz, DMSO-d_6): δ = 11.25 (2H, NH), 8.14–9.14 (6H, Ar–H), 7.09, 7.14 (2H, HC=N), 1.93 (3H, CH_3), 4.35 (1H, OH methanol) ppm; ^{13}C NMR (75 MHz, DMSO-d_6): δ = 174.89 (C=O), 158.50 (C=N), 138.93 (C1), 127.81 (C4), 124.62 (C5), 122.92 (C3), 121 (C6), 118.73 (C2) ppm; UV–Vis (Nujol mull): λ_{max} = 509 nm.

[2,2′-[Carbonylbis(hydrazin-2-yl-1-ylidenemethylidyne)]-bis(4-nitrophenolato)](8-hydroxyquinoline)-dioxouranium(VI) (**5**, $C_{24}H_{17}N_7O_{10}U$)

Uranyl acetate dihydrate ($UO_2(OAc)_2\cdot 2H_2O$, 0.547 g, 1.29 mmol) in 30 cm^3 methanol was added gradually with constant stirring to the solution of 0.5 g of the ligand H_2L^1 (1.29 mmol) in 30 cm^3 methanol. The reaction mixture was heated to reflux for 0.5 h then a methanolic solution of 0.187 g 8-hydroxyquinoline (1.29 mmol) was added and the

Table 5 Minimum inhibitory concentration of some synthesized compounds

Compound	Minimum inhibitory concentration/μg cm^{-3}					
	Gram-positive bacteria		Gram-negative bacteria		Yeasts and fungi	
	Staphylococcus aureus	*Bacillus subtilis*	*Salmonella typhimurium*	*Escherichia coli*	*Candida albicans*	*Aspergillus fumigatus*
H_2L^1	80	70	74	110	50	50
$[(L^1)VO]\cdot 4H_2O$ (**1**)	ND	15	ND	ND	7	8
$[(L^1)UO_2]\cdot 2MeOH$ (**4**)	60	18	18	68	30	38
$[(L^1)UO_2(8\text{-HQ})]$ (**5**)	2	4	15	6	2	1
$[(HL^1)UO_2(Gly)]\cdot 0.5MeOH$ (**6**)	ND	40	ND	ND	ND	ND
$[(L^1)UO_2(Sal)]\cdot 4H_2O$ (**7**)	ND	36	ND	ND	30	ND
$[(HL^1)UO_2(Bac)]\cdot MeOH$ (**8**)	ND	9	ND	44	26	ND
H_2L^2	77	66	70	100	44	45
$[(L^2)VO]\cdot 3H_2O$ (**9**)	16	8	ND	44	6	ND
$[(L^2)UO_2]\cdot 2H_2O$ (**12**)	70	41	66	45	31	36
$[(L^2)UO_2(8\text{-HQ})]\cdot 3H_2O$ (**13**)	64	40	18	45	30	8
$[(HL^2)UO_2(Gly)]\cdot 0.5H_2O$ (**14**)	70	40	ND	43	ND	ND
$[(L^2)UO_2(Sal)]\cdot H_2O$ (**15**)	67	39	ND	ND	ND	ND
$[(HL^2)UO_2(Bac)]\cdot H_2O$ (**16**)	69	42	ND	ND	ND	ND
Control[a]	9	1	13	41	3	2

ND not determined

[a] Chloramphenicol in the case of Gram-positive bacteria, cephalothin in the case of Gram-negative bacteria, and cycloheximide in the case of yeasts and fungi

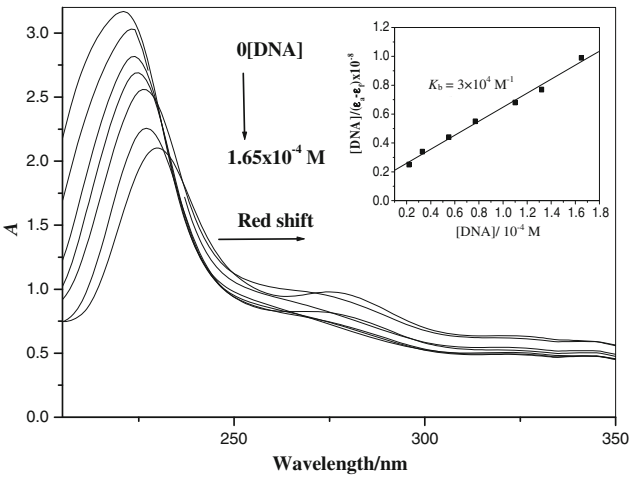

Fig. 7 Absorption spectra of the oxovanadium(IV) complex **9** in Tris–HCl buffer upon addition of different concentrations from HS-DNA; [complex] = 1×10^{-4} M, [DNA] = 0–1.65×10^{-4} M. *Insert* plot of $[DNA]/\varepsilon_a - \varepsilon_f$ vs. [DNA] for absorption titration of HS-DNA with the complex

resulting mixture was heated to reflux for 6 h. A brown precipitate was formed, filtered off, and washed several times with small amounts of methanol then diethylether, and finally air-dried. The yield was 0.72 g (70 %). M.p.: > 300 °C; IR (KBr): $\bar{\nu}$ = 3,422 (OH), 3,276 (NH), 1,636 (C=O), 1,605 (C=N), 1,574 (C=C), 1,312 $(C–O)_{phenolic}$, 517 (M–O), 440 (M–N), 899 (UO_2), 1,499 (C=N) 8H-Q cm^{-1}; ^1H NMR (300 MHz, DMSO-d_6): δ = 11.25 (2H, NH), 7.13–9.34 (12H, Ar–H), 7.09, 7.12 (2H, HC=N), 10.75 (1H, OH of 8-HQ) ppm; ^{13}C NMR (75 MHz, DMSO-d_6): δ = 175.0 (C=O), 155.02 (C=N), 137.81 (C1), 129.25 (C4), 123.59 (C5), 119.48 (C3), 118.71 (C6) and 113.02 (C2)(aromatic carbon atoms), 153 (C8), 149.9 (C2), 140.21 (C8a), 132 (C4), 130.54 (C4a), 125.0 (C6), 117 (C3), 114.5 (C5) and 109.0 (C7) (8-HQ); UV–Vis (Nujol mull): λ_{max} = 510 nm; MS (70 eV): *m/z* = 801 (M^+).

[2,2′-[Carbonylbis(hydrazin-2-yl-1-ylidenemethylidyne)]-bis(4-nitrophenolato)]oxovanadium(IV) tetrahydrate
(**1**, $C_{15}H_{18}N_6O_{12}V$)
M.p.: >300 °C; IR (KBr): $\bar{\nu}$ = 3,385 (OH), 3,215 (NH), 1,625 (C=O), 1,605 (C=N), 1,559 (C=C), 1,296 $(C–O)_{phenolic}$, 516 (M–O), 438 (M–N), 954 (VO) cm^{-1}; UV–Vis (Nujol mull): λ_{max} = 548 nm; MS (70 eV): *m/z* = 453 (M^+−4 H_2O).

[2,2′-[Carbonylbis(hydrazin-2-yl-1-ylidenemethylidyne)]-bis(4-nitrophenolato)](ethanol)cerium(III) nitrate·EtOH
(**2**, $C_{19}H_{22}N_7O_{12}Ce$)
M.p.: >300 °C; IR (KBr): $\bar{\nu}$ = 3,420 (OH), 3,231 (NH), 1,636 (C=O), 1,592 (C=N), 1,558 (C=C), 1,295 (C–

Table 6 Optical properties of oxovanadium(IV) complexes with the addition of DNA and their DNA binding constants

Complex	Absorption band maxima (nm)		Hypochromism/%	Red shift $\Delta\lambda$/nm	K_b/M^{-1}
	Free	Bound			
1	221	229	32.7	8	2.55×10^4
9	221	230	33.8	9	3×10^4

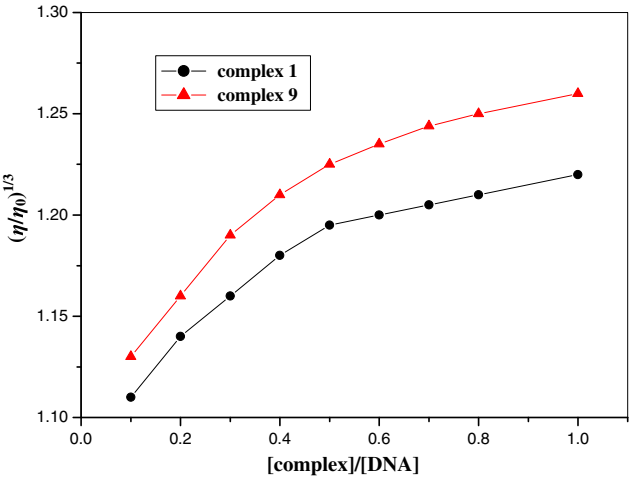

Fig. 8 Effect of increasing amounts of the oxovanadium(IV) complexes **1** and **9** on the relative viscosity of HS-DNA at 25.00 ± 0.01 °C

O)$_{phenolic}$, 506 (M–O), 460 (M–N), 1,423 (NO_3^-) cm^{-1}; UV–Vis (Nujol mull): λ_{max} = 502 nm.

[2,2′-[Carbonylbis(hydrazin-2-yl-1-ylidenemethylidyne)]-bis(4-nitrophenolato)]dinitratothorium(IV)·EtOH monohydrate (**3**, $C_{17}H_{18}N_8O_{15}Th$)
M.p.: >300 °C; IR (KBr): $\bar{\nu}$ = 3,420 (OH), 3,246 (NH), 1,636 (C=O), 1,607 (C=N), 1,559 (C=C), 1,316 (C–O)$_{phenolic}$, 507 (M–O), 423 (M–N), 1,384, 1,203 (NO_3^-) cm^{-1}; ^{1}H NMR (300 MHz, DMSO-d_6): δ = 9.20 (2H, NH), 7.88–8.47 (6H, Ar–H), 7.25, 7.30 (2H, HC=N), 1.97 (3H, CH_3), 1.22 (2H, CH_2), 4.65 (1H, OH of ethanol) ppm; UV–Vis (Nujol mull): λ_{max} = 452 nm.

[2,2′-[Carbonylbis(hydrazin-2-yl-1-ylidenemethylidyne)]-bis(4-nitrophenolato)](glycinato)dioxouranium(VI)·0.5 MeOH (**6**, $C_{17.5}H_{17}N_7O_{11.5}U$)
M.p.: >300 °C; IR (KBr): $\bar{\nu}$ = 3,446 (OH), 3,227 (NH), 1,644 (C=O), 1,600 (C=N), 1,569 (C=C), 1,308 (C–O)$_{phenolic}$, 592 (M–O), 490 (M–N), 886 (UO_2), 1,516, 1,362 (COO of Gly) cm^{-1}; UV–Vis (Nujol mull): λ_{max} = 508 nm.

[2,2′-[Carbonylbis(hydrazin-2-yl-1-ylidenemethylidyne)]-bis(4-nitrophenolato)](salicylaldehyde)dioxouranium(VI) tetrahydrate (**7**, $C_{22}H_{24}N_6O_{15}U$)
M.p.: >300 °C; IR (KBr): $\bar{\nu}$ = 3,434 (OH), 3,269 (NH), 1,641 (C=O), 1,604 (C=N), 1,564 (C=C), 1,306 (C–O)$_{phenolic}$, 532 (M–O), 499 (M–N), 903 (UO_2) cm^{-1}; UV–Vis (Nujol mull): λ_{max} = 506 nm.

(Benzoylacetonato)[2,2′-[Carbonylbis(hydrazin-2-yl-1-ylidenemethylidyne)]bis(4-nitrophenolato)]dioxouranium(VI)·MeOH (**8**, $C_{26}H_{24}N_6O_{12}U$)
M.p.: >300 °C; IR (KBr): $\bar{\nu}$ = 3,432 (OH), 3,310 (NH), 1,658 (C=O), 1,587 (C=N), 1,532 (C=C), 1,308 (C–O)$_{phenolic}$, 530 (M–O), 489 (M–N), 892 (UO_2) cm^{-1}; UV–Vis (Nujol mull): λ_{max} = 455 nm.

[1,1′-[Carbonylbis(hydrazin-2-yl-1-ylidenemethylidyne)]bis(naphthalen-2-olato)]-oxovanadium(IV) trihydrate (**9**, $C_{23}H_{22}N_4O_7V$)
M.p.: >300 °C; IR (KBr): $\bar{\nu}$ = 3,447 (OH), 3,215 (NH), 1,619 (C=O), 1,597 (C=N), 1,545 (C=C), 1,339 (C–O)$_{phenolic}$, 510 (M–O), 454 (M–N), 980 (VO) cm^{-1}; UV–Vis (Nujol mull): λ_{max} = 541 nm.

[1,1′-[Carbonylbis(hydrazin-2-yl-1-ylidenemethylidyne)]bis(naphthalen-2-olato)]-nitratocerium(III) 2.5-hydrate (**10**, $C_{23}H_{21}N_5O_{8.5}Ce$)
M.p.: >300 °C; IR (KBr): $\bar{\nu}$ = 3,420 (OH), 3,215 (NH), 1,618 (C=O), 1,592 (C=N), 1,540 (C=C), 1,340 (C–O)$_{phenolic}$, 546 (M–O), 458 (M–N), 1,360, 1,058 (NO_3^-) cm^{-1}; UV–Vis (Nujol mull): λ_{max} = 521 nm.

[1,1′-[Carbonylbis(hydrazin-2-yl-1-ylidenemethylidyne)]bis(naphthalen-2-olato)]-dinitratothorium(IV) tetrahydrate (**11**, $C_{23}H_{24}N_6O_{13}Th$)
M.p.: >300 °C; IR (KBr): $\bar{\nu}$ = 3,420 (OH), 3,169 (NH), 1,618 (C=O), 1,601 (C=N), 1,542 (C=C), 1,341 (C–O)$_{phenolic}$, 553 (M–O), 472 (M–N), 1,360, 1,063 (NO_3^-) cm^{-1}; ^{1}H NMR (300 MHz, DMSO-d_6): δ = 11.0 (2H, NH), 7.12–8.90 (12H, Ar–H), 9.20, 9.60 (2H, HC=N) ppm; UV–Vis (Nujol mull): λ_{max} = 460 nm; MS (70 eV): *m/z* = 752 (M^+−4 H_2O).

[1,1′-[Carbonylbis(hydrazin-2-yl-1-ylidenemethylidyne)]bis(naphthalen-2-olato)]-dioxouranium(VI) dihydrate (**12**, $C_{23}H_{20}N_4O_7U$)
M.p.: >300 °C; IR (KBr): $\bar{\nu}$ = 3,500 (OH), 3,245 (NH), 1,646 (C=O), 1,599 (C=N), 1,547 (C=C), 1,336 (C–O)$_{phenolic}$, 554 (M–O), 477 (M–N), 898 (UO_2) cm^{-1}; ^{1}H NMR (300 MHz, DMSO-d_6): δ = 13.56 (2H, NH), 7.33–9.22 (12H, Ar–H), 9.87, 10.05 (2H, HC=N) ppm; ^{13}C NMR (75 MHz, DMSO-d_6): δ = 173.55 (C=O), 168.82 (C=N), 159.26 (C2), 146.08 (C8a), 131.28 (C4), 128.77 (C4a), 127.73 (C5), 126.91 (C7), 122.25 (C8),

120.12 (C6), 118.66 (C3), 109.51 (C1) ppm; UV–Vis (Nujol mull): $\lambda_{max} = 465$ nm.

[1,1′-[Carbonylbis(hydrazin-2-yl-1-ylidenemethylidyne)]bis(naphthalen-2-olato)]-(8-hydroxyquinoline)dioxouranium(VI) trihydrate (**13**, $C_{32}H_{29}N_5O_9U$)
M.p.: >300 °C; IR (KBr): $\bar{\nu} = 3{,}576$ (OH), 3,271 (NH), 1,666 (C=O), 1,605 (C=N), 1,545 (C=C), 1,343 $(C–O)_{phenolic}$, 534 (M–O), 483 (M–N), 889 (UO_2), 1,497 (C=N) 8H-Q cm^{-1}; ^1H NMR (300 MHz, DMSO-d_6): $\delta = 11.95$, 11.64 (2H, NH), 7.08–9.97 (18H, Ar–H), 10.46, 10.35 (2H, HC=N), 11.08 (1H, OH of 8-HQ) ppm; ^{13}C NMR (75 MHz, DMSO-d_6): $\delta = 168.48$ (C=O), 167.45 (C=N), 157.25 (C2), 145.92 (C8a), 131.41 (C4), 145.92 (C8a), 131.41 (C4), 127.59 (C5), 127.31 (C7), 122.24 (C8), 120.05 (C6), 118.64 (C3) and 109.41 (C1) (aromatic carbon atom), 153.24 (C8), 150.61 (C2), 138.98 (C8a), 134 (C4), 129.88 (C4a), 122.47 (C6), 121.77 (C3), 114.76 (C5) and 113.91 (C7) (8-HQ) ppm; UV–Vis (Nujol mull): $\lambda_{max} = 447$ nm.

[1,1′-[Carbonylbis(hydrazin-2-yl-1-ylidenemethylidyne)]bis(naphthalen-2-olato)]-(glycinato)dioxouranium(VI) 0.5-hydrate (**14**, $C_{25}H_{22}N_5O_{7.5}U$)
M.p.: >300 °C; IR (KBr): $\bar{\nu} = 3{,}500$ (OH), 3,273 (NH), 1,618 (C=O), 1,598 (C=N), 1,544 (C=C), 1,340 $(C–O)_{phenolic}$, 554 (M–O), 482 (M–N), 885 (UO_2), 1,510, 1,300 (COO of Gly) cm^{-1}; ^1H NMR (300 MHz, DMSO-d_6): $\delta = 10.19$ (1H, OH), 9.85 (2H, NH), 7.27–8.14 (12H, Ar–H), 9.20 (2H, HC=N), 10.04 (2H, NH_2, Gly) 1.91 (2H, CH_2, Gly) ppm; UV–Vis (Nujol mull): $\lambda_{max} = 449$ nm.

[1,1′-[Carbonylbis(hydrazin-2-yl-1-ylidenemethylidyne)]bis(naphthalen-2-olato)]-(salicylaldehyde)dioxouranium(VI) hydrate (**15**, $C_{30}H_{24}N_4O_8U$)
M.p.: >300 °C; IR (KBr): $\bar{\nu} = 3{,}431$ (OH), 3,245 (NH), 1,615 (C=O), 1,596 (C=N), 1,461 (C=C), 1,338 $(C–O)_{phenolic}$, 545 (M–O), 479 (M–N), 893 (UO_2) cm^{-1}; ^1H NMR (300 MHz, DMSO-d_6): $\delta = 9.85$ (2H, NH), 7.24–8.33 (16H, Ar–H), 9.19, 9.50 (2H, HC=N), 11.0 (1H, OH, Sal) ppm; UV–Vis (Nujol mull): $\lambda_{max} = 436$ nm.

(Benzoylacetonato)[1,1′-[Carbonylbis(hydrazin-2-yl-1-ylidenemethylidyne)]bis(naphthalen-2-olato)]-dioxouranium(VI) hydrate (**16**, $C_{33}H_{28}N_4O_8U$)
M.p.: >300 °C; IR (KBr): $\bar{\nu} = 3{,}433$ (OH), 3,277 (NH), 1,611 (C=O), 1,555 (C=N), 1,460 (C=C), 1,344 $(C–O)_{phenolic}$, 547 (M–O), 476 (M–N), 898 (UO_2) cm^{-1}; ^1H NMR (300 MHz, DMSO-d_6): $\delta = 10.05$ (1H, OH), 9.85 (2H, NH), 7.25–8.17 (17H, Ar–H), 9.20 (2H, HC=N), 2.74 (3H, CH_3 of Bac) ppm; UV–Vis (Nujol mull): $\lambda_{max} = 443$ nm.

Unsuccessful trials

Several attempts to isolate the mixed-ligand complexes of the ligands H_2L^1 and H_2L^2 as primary ligands with dioxouranium(VI) ion in the presence of 2,2′-bipyridyl as a secondary ligand were unsuccessful. These attempts gave binary complexes.

Antimicrobial activity

The standardized disc–agar diffusion method [107, 108] was followed to determine the activity of the synthesized compounds against the sensitive organisms *Staphylococcus aureus* (ATCC 25923) and *Bacillus subtilis* (ATCC 6635) as Gram-positive bacteria, *Salmonella typhimurium* (ATCC 14028) and *Escherichia coli* (ATCC 25922) as Gram-negative bacteria, yeast *Candida albicans* (ATCC 10231), and fungus *Aspergillus fumigatus*. The antibiotic chloramphenicol was used as reference in the case of Gram-positive bacteria, cephalothin in the case of Gram-negative bacteria, and cycloheximide in the case of yeasts and fungi.

Screening for the antimicrobial potential

Preparation of tested compounds
The tested compounds were dissolved in dimethylformamide (DMF) and prepared in two concentrations: 100 and 50 mg/cm^3 and then 10 mm^3 of each preparation was dropped on disc of 6 mm in diameter and the concentrations became 1 and 0.5 mg/disc, respectively. In the case of insoluble compounds, the compounds were suspended in DMF and vortexed then processed.

Testing for anti-bacterial and yeasts activity
Bacterial cultures were grown in nutrient broth medium at 30 °C. After 16 h of growth, each microorganism, at a concentration of 10^8 cells/cm^3, was inoculated on the surface of Mueller–Hinton agar plates using sterile cotton swab. Subsequently, uniform-size filter paper discs (6 mm in diameter) were impregnated by equal volume (10 mm^3) from the specific concentration of dissolved compounds and carefully placed on surface of each inoculated plate. The plates were incubated in the upright position at 36 °C for 24 h. Three replicates were carried out for each extract against each of the test organism. Simultaneously, addition of the respective solvent instead of dissolved compound was carried out as negative controls. After incubation, the diameters of the growth inhibition zones formed around the disc were measured with transparent ruler in millimeter, averaged, and the mean values were tabulated.

Testing for anti-fungal activity
Active inoculum for experiments was prepared by transferring many loopfuls of spores from the stock cultures to

test tubes of sterile distilled water (SDW) that were agitated and diluted with sterile distilled water to achieve optical density corresponding to 2.0×10^5 spore/cm^3. Inoculum of 0.1 % suspension was swabbed uniformly and the inoculum was allowed to dry for 5 min then the same procedure was followed as described above.

Determination of minimum inhibitory concentration (MIC)
Minimum inhibitory concentration is the lowest concentration of an antimicrobial compound that will inhibit the visible growth of a microorganism after overnight incubation.

MIC values of the synthesized compounds were determined using agar dilution technique [109]. Each compound with an antimicrobial effect shown in the disc diffusion test was further diluted with DMF to 25.6, 12.8, 6.4, 3.2, 1.6, 0.8, 0.4, 0.2, and 0.1 mg/cm^3, respectively. The concentrations of the compounds became 256, 128, 64, 32, 16, 8, 4, 2, and 1 μg/cm^3, respectively. Then, 100 mm^3 of each diluted compound was mixed with 10 cm^3 of cooled (50 °C) melted Mueller–Hinton agar and 10 mm^3 of specific microbial culture (at concentration of 10^8 cells/cm^3) which were grown in nutrient broth medium for 16 h at 30 °C then plated into 6-cm sterile Petri dish. Each dilution was prepared in duplication. Each concentration was prepared for two dishes. All plates were incubated at 33 °C for 24 h. MIC of each compound was measured from the plate with the lowest concentration with no visible growth of specific organism.

DNA binding affinity of oxovanadium(IV) complexes

Absorption spectra method
All experiments involving herring sperm DNA (HS-DNA) were performed in tris(hydroxymethyl)aminomethane–HCl (Tris–HCl) buffer solution (pH 7.23), prepared using deionized water. Solutions of DNA in Tris–HCl buffer gave a ratio of UV absorbance at 260 and 280 nm, A_{260}/A_{280}, of ca. 1.9, indicating that the DNA was sufficiently free of protein [110]. The concentration of HS-DNA was determined from its absorbance at 260 nm using $\varepsilon_{260} = 6{,}600$ mol^{-1} dm^3 cm^{-1} [111]. Stock solutions of DNA were stored at 277 K and used after no more than 4 days. A concentrated stock solution of the oxovanadium(IV) complexes was prepared by dissolving the oxovanadium(IV) complex in DMF and diluting suitably with Tris–HCl buffer to required concentrations for all the experiments (1 % DMF and 99 % Tris–HCl). The absorption spectral titration experiment was performed by keeping the concentration of the complex constant and varying HS-DNA concentration. Equal volumes of solutions of HS-DNA were added to the complex and reference solutions to eliminate the absorbance of HS-DNA itself.

Viscosity measurements
Viscosity measurements were carried on an Ubbelohde viscometer in a thermostated water-bath maintained at 25.00 ± 0.01 °C. DNA concentration was kept constant (1×10^{-5} M) and gradually increased the concentration of oxovanadium(IV) complexes (1×10^{-6} to 1×10^{-5} M). HS-DNA samples approximately 200 base pairs in length were prepared by sonication to minimize complexities arising from DNA flexibility [112]. Flow times were measured with a digital stopwatch. Each sample was measured three times, and an average flow time was calculated. Relative viscosities for HS-DNA in the presence and absence of the complex were calculated from the relation $\eta = (t - t_0)/t_0$, where t is the observed flow time of DNA-containing solution and t_0 is that of Tris–HCl buffer alone. Data were presented as $(\eta/\eta_0)^{1/3}$ versus binding ratio [113], where η is the viscosity of HS-DNA in the presence of the oxovanadium(IV) complex and η_0 is the viscosity of DNA alone.

Acknowledgments The Authors are grateful to Prof. Dr. M.M. Mashaly and Dr. M. Saif, providing facilities to carry out DNA studies.

References

1. Harinath Y, Reddy DHK, Kumar BN, Apparao CH, Seshaiah K (2013) Spectrochim Acta A 101:264
2. Sedaghat T, Tahmasbi L, Motamedi H, Reyes-Martinez R, Morales-Morales D (2013) J Coord Chem 66:712
3. Abu El-Reash GM, El-Gammal OA, Radwan AH (2014) Spectrochim Acta A 121:259
4. Abu El-Reash GM, El-Gammal OA, Ghazy SE, Radwan AH (2013) Spectrochim Acta A 104:26
5. El-Gammal OA, Abu El-Reash GM, Ghazy SE, Radwan AH (2012) J Mol Struct 1020:6
6. Eswaran S, Adhikari AV, Pal NK, Chowdhury IH (2010) Bioorg Med Chem Lett 20:1040
7. Reddy KH, Reddy PS, Babu PR (2000) Trans Met Chem 25:505
8. Joshi JD, Sharma S, Patel G, Vora JJ (2002) Synth React Inorg Met Org Chem 32:1729
9. Subbaraj P, Ramu A, Raman N, Dharmaraja J (2014) Spectrochim Acta A 117:65
10. Dharmaraja J, Esakkidurai T, Subbaraj P, Shobana S (2013) Spectrochim Acta A 114:607
11. Aljahdali M, El-Sherif AA (2013) Inorg Chim Acta 407:58
12. Abu Ali H, Darawsheh MD, Rappocciolo E (2013) Polyhedron 61:235
13. Shobana S, Dharmaraja J, Selvaraj S (2013) Spectrochim Acta A 107:117
14. Sampath K, Sathiyaraj S, Raja G, Jayabalakrishnan C (2013) J Mol Struct 1046:82
15. Mashaly MM, El-Shafiy HF, El-Maraghy SB, Habib HA (2005) Spectrochim Acta A 61:1869
16. Mishra AP, Soni M (2008) Met Based Drugs 10:1
17. Dong Y, Narla RK, Sudbeck E, Uckun FM (2000) J Inorg Biochem 78:321
18. Noblia P, Vieites M, Parajon-Costa BS, Baran EJ, Cerecetto H, Draper P, Gonzalez M, Piro OE, Castellano EE, Azqueta A,

Cerain AL, Monge-Vega A, Gambino D (2005) J Inorg Biochem 99:443
19. Szacilowski K, Macyk W, Drzewiecka-Matuszek A, Brindell M, Stochel G (2005) Chem Rev 105:2647
20. Sakurai H, Kojitane Y, Yoshikawa Y, Kawabe K, Yasui H (2002) Coord Chem Rev 226:187
21. Cotton SA (1999) Polyhedron 18:1691
22. Meehan PR, Aris DR, Willey GR (1999) Coord Chem Rev 181:121
23. Drozdzynski J (2005) Coord Chem Rev 249:2351
24. Sessler JL, Melfi PJ, Pantos GD (2006) Coord Chem Rev 250:816
25. Bunzli J-CG, Piquet C (2002) Chem Rev 102:1897
26. Bunzli J-CG (2006) Acc Chem Res 39:53
27. Zhao P, Xu LC, Huang JW, Zheng KC, Liu J, Yu HC, Ji LN (2008) Biophys Chem 134:72
28. Dhar S, Nethaji M, Charkravarty AR (2005) Inorg Chem 44:8876
29. Kumar RS, Arunachalam S (2008) Biophys Chem 136:136
30. Alaghaz AMA, El-Sayed BA, El-Henawy AA, Ammar RAA (2013) J Mol Struct 1035:83
31. Karastogianni S, Dendrinou-Samara C, Ioannou E, Raptopoulou CP, Hadjipavlou-Litina D, Girousi S (2013) J Inorg Biochem 118:48
32. Pathan AH, Bakale RP, Naik GN, Frampton CS, Gudasi KB (2012) Polyhedron 34:149
33. Kulkarni NV, Kamath A, Budagumpi S, Revankar VK (2011) J Mol Struct 1006:580
34. Benítez J, de Queiroz AC, Correia I, Alves MA, Alexandre-Moreira MS, Barreiro EJ, Lima LM, Varela J, González M, Cerecetto H, Moreno V, Pessoa JC, Gambino D (2013) Eur J Med Chem 62:20
35. Li L, Guo Z, Zhang Q, Xu T, Wang D (2010) Inorg Chem Commun 13:1166
36. Banik B, Somyajit K, Koley D, Nagaraju G, Chakravarty AR (2012) Inorg Chim Acta 393:284
37. Prasad P, Sasmal PK, Khan I, Kondaiah P, Chakravarty AR (2011) Inorg Chim Acta 372:79
38. Abu-Hussen AAA, Emara AAA (2004) J Coord Chem 57:973
39. Lever ABP (1984) Inorganic electronic spectroscopy, 2nd edn. Elsevier, Amsterdam
40. Shrivastav A, Singh NK, Tripathi P, George T, Dimmock JR, Sharma RK (2006) Biochimie 88:1209
41. Shebl M (2008) Spectrochim Acta A 70:850
42. Shebl M, Ibrahim MA, Khalil SME, Stefan SL, Habib H (2013) Spectrochim Acta A 115:399
43. Shebl M (2009) J Coord Chem 62:3217
44. Seleem HS, El-Shetary BA, Khalil SME, Mostafa M, Shebl M (2005) J Coord Chem 58:479
45. Shebl M, Khalil SME, Taha A, Mahdi MAN (2013) Spectrochim Acta A 113:356
46. Shebl M, Khalil SME, Taha A, Mahdi MAN (2012) J Am Sci 8:183
47. Soliman AA, Mohamed GG (2004) Thermochim Acta 421:151
48. Chandra S, Pundir M (2007) Spectrochim Acta A 68:833
49. Saif M, Mashaly MM, Eid MF, Fouad R (2012) Spectrochim Acta A 92:347
50. Shebl M, Khalil SME, Ahmed SA, Medien HAA (2010) J Mol Struct 980:39
51. Khalil SME, Shebl M, Al-Gohani FS (2010) Acta Chim Slov 57:716
52. Shebl M (2009) Spectrochim Acta A 73:313
53. Khalil SME, Seleem HS, El-Shetary BA, Shebl M (2002) J Coord Chem 55:883
54. Shebl M, Khalil SME, Al-Gohani FS (2010) J Mol Struct 980:78
55. McGlynn SP, Smith JK, Neely WC (1961) J Chem Phys 35:105
56. Jones LH (1958) Spectrochim Acta A 10:395
57. Selbin LHH, McGlynn SP (1963) J Inorg Nucl Chem 25:1359
58. El-Asmy AA, El-Gammal OA, Radwan HA, Ghazy SE (2010) Spectrochim Acta A 77:297
59. Shebl M (2014) Spectrochim Acta A 117:127
60. Geary WJ (1971) Coord Chem Rev 7:81
61. El-Metwally NM, El-Shazly RM, Gabr IM, El-Asmy AA (2005) Spectrochim Acta A 61:1113
62. Khalil SME, El-Shafiy HFO (2000) Synth React Inorg Met Org Chem 30:1817
63. Sarrano CJ, Bonadies JA (1986) J Am Chem Soc 108:4088
64. Ooi S, Nishizawa M, Matasuto K, Kuroya H, Saito K (1979) Bull Chem Soc Jpn 52:452
65. Shebl M, Seleem HS, El-Shetary BA (2010) Spectrochim Acta A 75:428
66. Abd El-Wahab ZH, Mashaly MM, Salman AA, El-Shetary BA, Faheim AA (2004) Spectrochim Acta A 60:2861
67. Tarafder MTH, Ali AM, Wong YW, Wong SH, Crouse KA (2001) Synth React Inorg Met Org Chem 31:115
68. Ferenc W, Dziewulska AW (2001) J Serb Chem Soc 66:543
69. Zheng YQ, Zhou LX, Lin JL, Wei DY (2002) Z Naturforsch 57b:1244
70. Khalil SME (2003) J Coord Chem 56:1013
71. Mashaly MM, Abd El-Wahab ZH, Faheim AA (2004) J Chin Chem Soc 51:1
72. Sun W, Yuan G, Liu J, Ma L, Liu C (2013) Spectrochim Acta A 106:275
73. Patel DA, Patel AA, Patel HS (2013) Arab J Chem. doi:10.1016/j.arabjc.2013.07.056
74. Zhang-Lin Y, Forissier M, Vedrine JC, Volta JC (1994) J Catal 145:267
75. Bencini A, Gattechi D (1990) EPR of exchange coupled systems. Springer, Berlin
76. Abou-Hussen AA, El-Metwally NM, Saad EM, El-Asmy AA (2005) J Coord Chem 58:1735
77. Yen TF (1969) Electron spin resonance of metal complexes, 1st edn. Plenum Press, New York
78. Mangalam NA, Kurup MRP (2009) Spectrochim Acta A 71:2040
79. Raman N, Kulandaisamy A, Jeyasubramanian K (2002) Synth React Inorg Met Org Chem 32:1583
80. Shebl M, Khalil SME, Taha A, Mahdi MAN (2012) J Mol Struct 1027:140
81. Seleem HS, El-Shetary BA, Shebl M (2007) Heteroatom Chem 18:100
82. Seleem HS, Emara AA, Shebl M (2005) J Coord Chem 58:1003
83. Quan CX, Bin LH, Bang GG (2005) Mater Chem Phys 91:317
84. Shirley R (2000) CRYSFIRE system for automatic powder indexing: user's manual. The Lattice Press, Guildford
85. Thimmaiah KN, Lloyd WD, Chandrappa GT (1985) Inorg Chim Acta 106:81
86. Chakrabarti P (1993) J Mol Biol 234:463
87. Khan TA, Naseem S, Khan SN, Khan AU, Shakir M (2009) Spectrochim Acta A 73:622
88. Anbu S, Kandaswamy M, Suthakaran P, Murugan V, Varghese B (2009) J Inorg Biochem 103:401
89. Chosh K, Kumar P, Tyagi N, Singh UP, Coel N, Chakraborty A, Roy P, Baratto MC (2011) Polyhedron 30:2667
90. Wang XL, Chao H, Hong XL, Liu YJ, Ji LN (2005) Trans Met Chem 30:305
91. Rompel A, Fischer H, Meiwes D, Karentzopoulos KB, Diillinger R, Tuczek F, Witzel H, Krebs B (1999) J Biol Inorg Chem 4:56
92. Gao F, Chao H, Zhou F, Yuan Y-X, Peng B, Ji LN (2006) J Inorg Biochem 100:1487
93. Barton JK, Danishefsky AT, Goldberg JM (1984) J Am Chem Soc 106:2172

94. Uma V, Kanthimathi M, Weyhermuller T, Nair BU (2005) J Inorg Biochem 99:2299
95. Anbu S, Kandaswamy M (2011) Polyhedron 30:123
96. Mudasir, Yoshioka N, Inoue H (1999) J Inorg Biochem 77:239
97. Shivakumar L, Shivaprasad K, Revanasiddappa HD (2012) Spectrochim Acta A 97:659
98. Lu J, Guo H, Zeng X, Zhang Y, Zhao P, Jiang J, Zang L (2012) J Inorg Biochem 112:39
99. Leelavathy L, Anbu S, Kandaswamy M, Karthikeyan N, Mohan N (2009) Polyhedron 28:903
100. Lu JZ, Du YF, Guo HW (2011) J Coord Chem 64:1229
101. McCrate A, Carlone M, Nielsen M, Swavey S (2010) Inorg Chem Commun 13:537
102. Chaires JB, Dattagupta N, Crothers DM (1982) Biochemistry 21:3933
103. Satyanarayana S, Dabrowiak JC, Chaires JB (1992) Biochemistry 31:9319
104. Jin L, Yang P (1997) J Inorg Biochem 68:79
105. Satyanarayana S, Dabrowiak JC, Chaires JB (1993) Biochemistry 32:2573
106. Mabbs FE, Machin DI (1973) Magnetism and transition metal complexes. Chapman and Hall, London
107. Bauer AW, Kirby WWM, Sherris JC, Turck M (1966) Am J Clin Pathol 45:493
108. Rahman AU, Choudhary MI, Thomsen WJ (2001) Bioassay techniques for drug development. Harwood Academic Publishers, The Netherlands
109. Andrews JM (2001) J Antimicrob Chemother 48:5
110. Marmur V (1961) J Mol Biol 3:208
111. Reichmann ME, Rice SA, Thomas CA, Doty PJ (1954) J Am Chem Soc 76:3047
112. Cohen G, Eisenberg H (1969) Biopolymers 8:45
113. Barton JK, Goldberg JM, Kumar CV, Turro NJ (1986) J Am Chem Soc 108:2081